Calcium Carbonate Formation in Water Distribution Systems and Autogenous Repair of Leaks by Inert Particle Clogging

Colin Scott Richards

Thesis submitted to the faculty of the Virginia Polytechnic Institute and State University in partial fulfillment of the requirements for the degree of

Master of Science
In
Civil and Environmental Engineering

Marc A. Edwards, Chair
Sunil K. Sinha
Fei Wang

May 2nd, 2016
Blacksburg, VA

Keywords: Calcium carbonate, distribution system, precipitation, particle clogging, autogenous repair

Calcium Carbonate Formation in Water Distribution Systems and Autogenous Repair of Leaks by Inert Particle Clogging

Colin Scott Richards

Abstract (academic)

The formation of calcium carbonate ($CaCO_3$) (i.e. scale) in potable water systems has long been a concern in water treatment and distribution. A literature review reveals that $CaCO_3$ scaling issues are re-emerging due to climate change, temperature increases in hot water systems and lower use of scaling and corrosion inhibitors. Moreover, we have gathered insights that suggest $CaCO_3$ coatings can be beneficial and stop pipeline leaks via self-repair or clogging. Ironically, the actions we are taking to increase the lifespan of distribution systems (i.e. adding corrosion inhibitors) might have worsened leaks and pipe lifespans due to interference with self-repair. The increasing occurrence of scaling coupled with gaps in knowledge over $CaCO_3$ formation in water systems make revisiting this topic timely.

The concept of autogenous repair by clogging with inert particles was examined using silica and alumina. Small 250 μm diameter pinhole leaks were simulated in bench-scale water recirculation systems. Silica and alumina particles were added to solutions ranging from high to low ionic strength to determine the impact of water quality on leak repair. Size distribution and zeta potential of the particles were measured. Silica particles were practically unchanged by the different solution chemistries while the size and zeta potential of alumina particles varied. The rate of clogging with silica particles was not impacted by water chemistry. Alumina particles with a positive charge clogged 100% of the leaks while negatively charged alumina could not clog 100%. Very small alumina particles (4.1 μm) stayed suspended but were unable to clog leaks.

Abstract (public)

Formation of calcium carbonate ($CaCO_3$) scale within water distribution and plumbing systems can cause major problems such as increased head loss and decreased energy efficiency in water heating systems. $CaCO_3$ scale formation in potable water was once believed to be fully understood in water treatment and distribution, however there are several emerging trends that are causing the problematic formation to re-emerge, such as climate change, temperature increases in hot water systems, and lower usage of corrosion inhibitors. $CaCO_3$ can also play a beneficial role in repairing leaks that form in pipelines by either depositing directly over the leak or by clogging the leak as a particle. Actions taken to lengthen the lifespan of water pipelines, such as adding corrosion and scaling inhibitors, may be having the opposite effect by preventing leak repair via $CaCO_3$.

The concept of leak repair by particle clogging was tested with alumina (Al_2O_3) and silica (SiO_2) particles approximately 10-100 μm in diameter. Circular leaks 250 μm in diameter were simulated using glass capillary tubing in water-recirculating systems. The particles were suspended in recirculating water and passed through the leaks. Water quality parameters such as pH and ionic strength were adjusted to assess the impact of water quality on repair rate; the SiO_2 particle characteristics were practically unchanged while Al_2O_3 characteristics varied. Al_2O_3 in lower pH solutions had significantly higher repair rates than Al_2O_3 in higher pH solutions. Very small Al_2O_3 particles (1.4 μm) were not able to clog leaks over a long period of time.

Acknowledgements

First, I am very grateful of my advisor Dr. Marc Edwards for his support, patience, and mentorship during my three years of graduate study. His incorruptible selflessness in sticking up for the public is something that will stay with me throughout my career as an engineer, and has made working with him a truly rewarding experience.

I would also like to thank my research colleagues Dr. Fei Wang and Min Tang, as well as the rest of the Edwards group, for helping me out with this project and giving me criticism when it was necessary. Thanks also to Dr. Sunil Sinha for his time serving on my committee. Dr. William Becker also deserves recognition for his support in writing and presenting the literature review.

Funding was provided by the NSF under grant CBET-1336616. My graduate studies were also partially supported by the Via Fellowship.

Attributions

Dr. Fei Wang - Post-doctoral researcher, Department of Civil and Environmental Engineering, Virginia Tech. Contributed section "1.5 Control and prevention of calcium carbonate scaling" to the literature review chapter, was involved in the organization and editing of Chapters 1 and 2, and helped in the creation of the tables and figures.

Dr. William Becker - Vice President of Water Process Research and Technology, Hazen and Sawyer. Provided results of autogenous repair pilot study on the Delaware Aqueduct, edited Chapter 1, and assisted in drawing of Figure 1-1.

Dr. Marc Edwards - Professor, Department of Civil and Environmental Engineering, Virginia Tech. Provided funding and guidance on research detailed in Chapter 2. Major contribution to the writing of Chapters 1 and 2.

Min Tang - Ph.D. candidate, Department of Civil and Environmental Engineering, Virginia Tech. Water recirculation systems described and Chapter 2 were influenced by the recirculating systems used in her research. Authored a literature review on autogenous repair of leaks that lead to this project.

Table of Contents

List of Figures

List of Tables

Chapter 1: Literature Review - A 21st Century Perspective on Calcium Carbonate Formation in Potable Water Systems

1.1 Introduction

The prediction, monitoring, and consequences of $CaCO_3$ formation have long been a key issue in potable water treatment. An early concern was that waters highly undersaturated with $CaCO_3$ would be corrosive to metallic and concrete pipe infrastructure (Baylis, 1935), and for waters highly supersaturated with $CaCO_3$, issues related to scaling (i.e., pipe clogging, head loss, higher heating costs) are the primary concerns (Garrett-Price et al., 1985). In the 80+ years since the landmark studies examining these issues were published, many changes have occurred that can profoundly alter the likelihood of $CaCO_3$ scaling in potable water systems including chemical corrosion control, changing water heater set-point temperatures, autogenous repair, global warming, biofilm growth, and erosion corrosion. This review is aimed at summarizing these changes and highlighting their practical implications for water utilities, regulators, building managers and consumers (Figure 1-1).

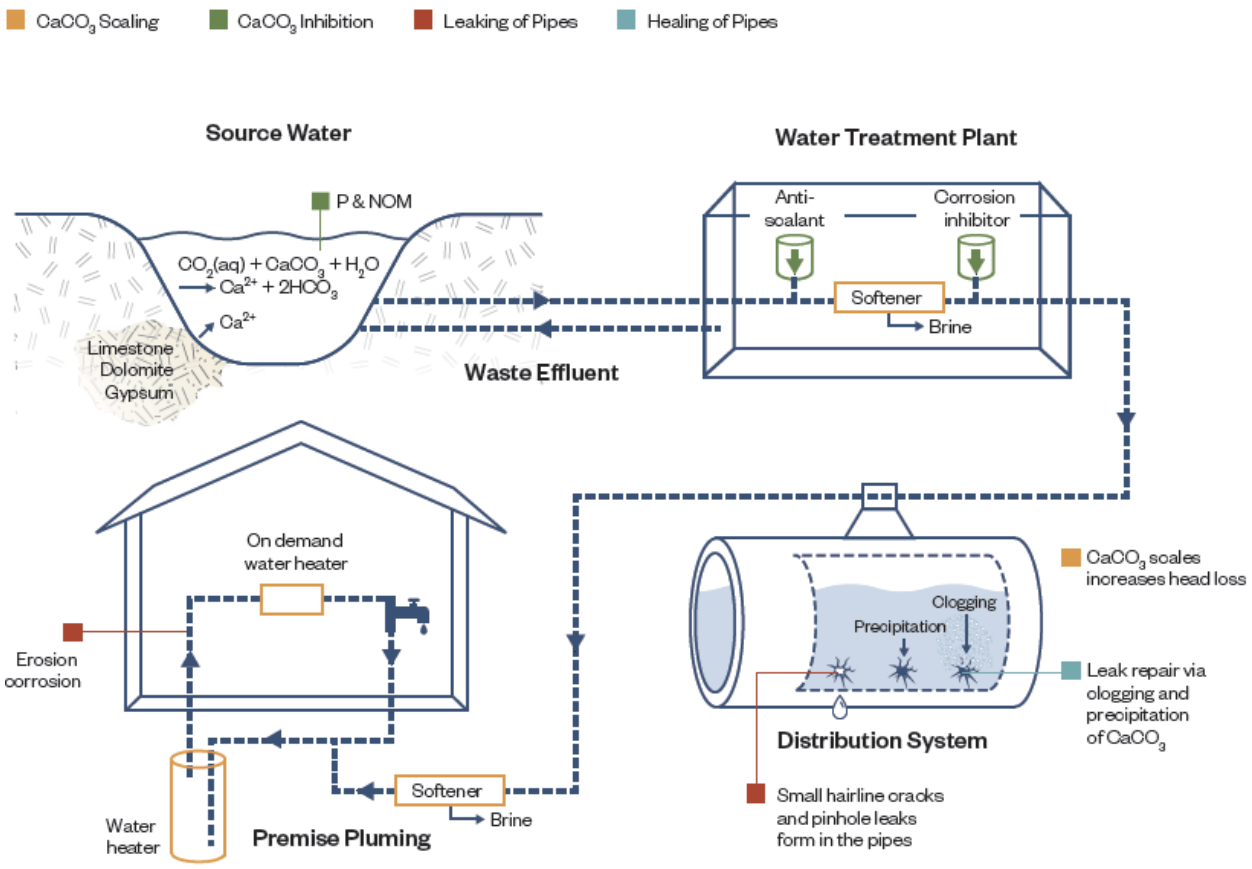

Figure 1-1 Overview of $CaCO_3$ from source to tap: Beneficial and detrimental impacts of $CaCO_3$ from source to tap. (1) Source water: Surface waters equilibrate with CO_2, controlling pH and adding inorganic carbon to the system. Natural inhibitors to $CaCO_3$ precipitation such as phosphate and NOM enter water through runoff or wastewater discharge, while calcium containing minerals in soils such as limestone can dissolve. (2) Water treatment plant: Corrosion inhibitors are also antiscalants that can inhibit $CaCO_3$ formation. Membrane softening processes often scale and produce a brine reject stream with high hardness and treated water with lower hardness. (3) Distribution system: $CaCO_3$ scale forms over distribution lines, protecting them from corrosive waters and potentially sealing leaks, but also increasing the head loss. (4) Premise plumbing: In households and buildings with ion exchange or RO membrane softeners, brine reject streams with high hardness are produced. Water heaters are very susceptible to scaling due to their high temperatures. Scale can easily coat heating elements and clog the narrow channels in on-demand water heaters. Particulate $CaCO_3$ may accelerate erosion corrosion.

1.1.1 Scaling

Scaling is the most obvious manifestation of $CaCO_3$ precipitation in potable water systems, resulting in flow restrictions in the system by clogging plumbing devices and creating head loss (Krappe, 1940; Crabtree et al., 1999). $CaCO_3$ scaling is a problem in granular media filters, where its formation can "cement" together the filter bed making it difficult to regenerate the media (Logsdon et al., 2002). Scaling is also a major issue in modern filters such as reverse osmosis (RO) or ultrafiltration membranes as it contributes to membrane fouling (Gwon et al., 2003). The concentration of Ca^{2+} and inorganic carbon in the reject stream can lead to $CaCO_3$ precipitating on the membrane surface (Bremere et al., 1999) and it is recommended that feed water pH is lowered to prevent scaling on the membrane and brine discharge system (Seneviratne, 2007).

The increased propensity of $CaCO_3$ to precipitate at higher temperatures makes scaling a troublesome issue in hot water systems, especially in water heater or water cooling applications in which scale layers interfere with heat transfer and system efficiency. Water heating is extremely energy intensive, and the total energy demand for building water heating systems exceeds the energy demand for the entire water and wastewater utility sector (Brazeau and Edwards, 2011). It is estimated that a hard water can lower the heat transfer efficiency of gas storage water heaters by 8.5%, and of instantaneous gas water heaters by 30%, over a 15 year lifecycle if no softening or de-liming is practiced (WQRF, 2011). Softening hard water can reduce the life cycle cost of instantaneous gas water heaters by 22.5% and gas storage water heaters by 6.6% over a 15 year lifecycle (WQRF, 2011). The annual cost of fouling for industrial operations in the U.S. alone was estimated in 1982 to be around $3-10 billion (Garrett-Price et al., 1985), including the cost of anti-scaling programs, downtime for maintenance, lost production, cleaning, higher energy costs due to reduced heat transfer, and over-sizing equipment where fouling is expected. The worldwide cost in 2000 was estimated at roughly $26 billion and $8-10 billion in the U.S. alone (Müller-Steinhagen, 2000).

1.1.2 Autogenous Repair

A possible but overlooked benefit of $CaCO_3$ formation in potable water systems is its ability to seal leaks in a process known as autogenous leak repair. This method may have been first

discovered and applied in ancient Rome, where the addition of alkaline wood ash was used to seal leaking pipelines (Pollio 15 BC as translated by Morgan, 1960). Although the mechanism of leak repair is unspecified, the high pH of wood ash solutions of 11.7-13.1 (Pitman, 2006) would also cause solids to precipitate in the water and clog leaks, in addition to the particulates in wood ash that could directly block leaks. In modern times the self-healing of concrete cracks and leaks is known to be critical to the satisfactory long-term performance of concrete structures and pipelines (Hearn, 1998; Edvardsen, 1999). Autogenous healing via hydration reactions in concrete have been frequently observed (Hearn, 1998). However, $CaCO_3$ deposition is also a major contributor to concrete repair (Edvardsen, 1999; Clear, 1985). Parks et al. (2010) found that concrete can also be repaired via magnesium-silicate precipitates which also form autogenously at higher pH in certain waters.

1.2 Recent Trends Affecting $CaCO_3$ Formation

Overview. In the last half-century, the science and practice of potable water treatment and distribution has changed markedly in ways that can profoundly alter the extent of $CaCO_3$ formation and scaling in water main and premise plumbing pipe systems (Figure 1-1). Inorganic carbon dissolves into natural water systems from CO_2 in the atmosphere, and Ca^{2+} is released in natural waters through dissolution of minerals such as portlandite, gypsum, and dolomite that come into contact with the water (Table 1-1). De-icing salt can also contribute thousands of tons of Ca^{2+} to groundwater in regions where calcium chloride is used (Houska, 2007).

Table 1-1: Solubility of calcium containing minerals found in natural waters

Mineral	pK_{sp} (25 °C)	Reaction	References
Limestone (calcite + aragonite)	8.34 - 8.48	$CaCO_3(s) \rightleftharpoons Ca^{2+} + CO_3^{2-}$	Plummer and Busenberg, 1982
Portlandite	22.8	$Ca(OH)_2(s) \rightleftharpoons Ca^{2+} + 2OH^-$	Brezonik and Arnold, 2011
Dolomite	17.2	$CaMg(CO_3)_2(s) + H^+ \rightleftharpoons MgCO_3(s) + Ca^{2+} + HCO_3^-$	Sherman and Barak, 2000
Gypsum	4.16	$CaSO_4 \cdot 2H_2O(s) \rightleftharpoons Ca^{2+} + SO_4^{2-} + 2H_2O$	Brezonik and Arnold, 2011

$CaCO_3$ formation as a corrosion control method has fallen out of favor. Corrosion has taken a heavy toll on plumbing and distribution systems throughout the U.S. The cost of maintaining the aging drinking water infrastructure in the U.S. alone will exceed $1 trillion over the next 25 years (AWWA, 2012). The original basis for controlling or reducing corrosion in potable water distribution systems was based on the premise that a layer of $CaCO_3$ formed on pipe surfaces could almost completely protect all pipe materials from corrosive reactants in the water supply including oxygen and free chlorine. Numerous corrosion indices based on this hypothesis were formulated to monitor and control the supposedly protective carbonate scales including: Langelier saturation index (LSI), Ryznar stability index (RSI), Puckorius scaling index (PSI), Larson-Skold index (LI), and measurement of temporary hardness (Langelier, 1936; Ryznar and Langelier, 1944; Puckorius and Brooke, 1991; Larson and Skold, 1958). Early on some of these indices were criticized because

they oversimplified the process of scaling (Wiggin et al., 1938; Schneider and Stumm, 1964). Such views dominated potable water treatment until about the mid-1980s, when researchers studying corrosion began to notice that iron, lead, and copper corrosion had little to do with $CaCO_3$ precipitation, and a consensus emerged that the overall approach was without basis and should be abandoned (Stumm, 1956; Larson and Skold, 1957; Schock, 1989; AWWARF, 1996). However, that consensus neglected to consider the possible benefits of the approach in reducing pipeline leaks and extending lifetime of assets through autogenous repair processes or clogging (Tang et al., 2013). In practice, many water utilities continue to calculate and target specific levels of $CaCO_3$ saturation (or undersaturation) for corrosion control.

$CaCO_3$ scaling in building heating systems has recently become an increased concern. Many buildings are now beginning to target higher hot water system temperature setpoints (> 51 °C) to reduce growth of pathogens (e.g. *Legionella pneumophila)*. Because the solubility of $CaCO_3$ decreases as temperature increases, and rates of precipitation also increase, scale formation on the surface of the heating element and throughout the system occurs more rapidly. Scaling can create serious problems including loss of heat transfer efficiency in heating systems, head loss (energy loss) induced by pipe clogging, and in some cases erosion corrosion from particles (Crabtree et al., 1999; Dobersek and Goricanec, 2007; Krappe, 1940; Roy and Edwards, 2015). Lower heat transfer efficiency in heating systems can severely impair the proper operation of water heaters in homes and buildings as well as cooling towers and heat exchangers in industrial settings (Garrett-Price et al., 1985).

Tankless on-demand water heaters are emerging as an important energy conserving device, due to their minimal hot water storage volumes and heat losses due to stagnation. The Department of Energy estimates that a centralized on-demand water heating system can reduce energy consumption by 8-34% (U.S. DoE) compared to conventional tank systems. Homeowners with gas heated on-demand systems are also eligible for federal tax credits (Energy Star) and the lack of stored hot water can reduce the risk of opportunistic pathogen growth (Brazeau and Edwards, 2011). Although these factors incentivize home and building owners to install on-demand water heaters, their high surface area-to-volume ratio at heat transfer surfaces, which are inherent to their instant heating design, makes them highly susceptible to $CaCO_3$ scaling and clogging in scaling

waters (Thomas et al., 2006; Brazeau and Edwards, 2011). In some cases, scaling may also reduce or eliminate their energy savings relative to conventional water heaters.

$CaCO_3$ may have the ability to clog leaks that have formed in pipes and extend the lifetime of distributions systems. It is hypothetically possible, that despite the sound scientific work discrediting Langelier and related indices as a guide to corrosion control, that the indices might have actually been "working" as advertised in controlling pipe leaks and extending distribution system lifetimes (DeMartini, 1938) but for reasons other than corrosion control. Specifically, rather than forming a thin $CaCO_3$ layer to protect pipe from corrosion and associated leaks (Langelier, 1936), it is possible that a high $CaCO_3$ formation potential could have reduced leak frequency by autogenous repair or clogging of leaks (Tang et al., 2013). Autogenous repair is a process by which existing leaks seal themselves, and $CaCO_3$ formation is a well-known leak self-repair mechanism for concrete pipes (Parks et al., 2010; Edvardsen, 1999). It is possible that this mechanism could also repair and heal leaks in metallic pipes before the leak holes grow to catastrophic failure, by either clogging of holes, assisting the formation of stronger or thicker pipe scales, or formation of corrosion byproducts (Tang et al., 2013; Tang et al., 2015). More research is needed correlating actual leaks to $CaCO_3$ formation potential to test this hypothesis, especially given the poor condition of U.S. distribution system assets and lack of financial resources for traditional repair and replacement.

$CaCO_3$ precipitation inhibitors that are naturally present or are added at the point of treatment have probably changed the propensity of water to form $CaCO_3$ scales in the last few decades. Water treatment policies aimed at controlling lead and copper corrosion dramatically increased the use of phosphate and polyphosphate corrosion inhibitors starting around 1990. These inhibitors are known to slow $CaCO_3$ precipitation kinetics in potable water systems (Lin and Singer, 2005a; Lin and Singer, 2006). Use of such corrosion inhibitors might prevent leak repair that occurs naturally for concrete pipe leaks or even possibly for metallic pipe leaks that would have occurred when the inhibitor was absent. On the other hand, this may be offset by increased removal of natural organic matter (NOM) that many plants are trying to achieve due to its role as a disinfection byproduct (DBP) precursor. NOM has been shown to inhibit $CaCO_3$ precipitation (Lin et al., 2005).

Climate change may play a role in $CaCO_3$ formation. Rising CO_2 levels in the atmosphere and more frequent and longer droughts caused by global warming can increase calcium levels in natural waters (Anderson and Faust, 1972; Mosley, 2015). Consequently, the $CaCO_3$ saturation index in potable water systems may also be rising (Figure 1-2). The net effect of these changes is as yet unclear. Some types of dissolved organic carbon (DOC) are known to be a $CaCO_3$ precipitation inhibitor (Lebron and Suarez, 1996). Although the major cause of increased DOC levels in natural waters is attributed to a decrease in acid rain deposition (Evans et al., 2006), there is evidence that higher CO_2 levels leading to increases in primary productivity (Freeman et al., 2004) and rising temperatures (Freeman et al., 2001) also contribute to DOC release.

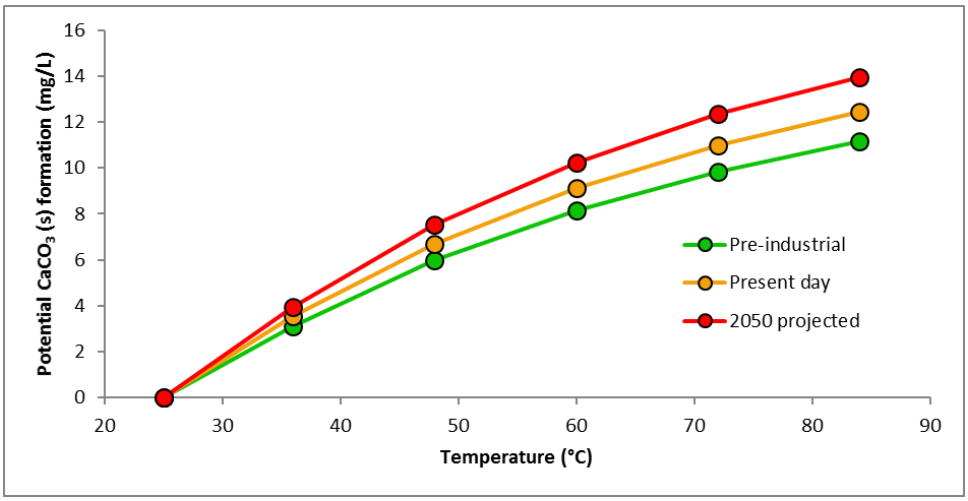

Figure 1-2 Impact of rising atmospheric CO_2 levels on $CaCO_3$ formation: Calcite at equilibrium with atmospheric CO_2 levels in the pre-industrial era, present day, and those projected for 2050. Higher atmospheric CO_2 can increase the precipitation potential. Using Mineql+, waters were equilibrated at $[Ca^{2+}]$ = 40 mg/L and P_{CO2} = $280x10^{-6}$, $390x10^{-6}$, and $550x10^{-6}$ atm. Using the equilibrium Ca_T, Alk, and pH from the open systems as starting conditions for the closed systems, the potential $CaCO_3$ formation at equilibrium was calculated for the closed systems.

Scaling has been shown to affect biofilm growth in premise plumbing.

A comprehensive study conducted by Fox and Abbaszadegan (2013) found that scale on PVC and copper, materials common in premise plumbing, promoted biofilm growth because it increased the surface roughness and provided a protected structure for the biofilm to grow on. An increase in

biofilm growth was most pronounced on scaled copper surfaces because the scale shielded the biofilm from the antimicrobial properties of copper.

Bulk precipitation of $CaCO_3$ may contribute to erosion corrosion in plumbing systems. Erosion corrosion occurs via mechanical action of fluid and suspended particles removing protective films on pipe surfaces. Roy and Edwards (2015) investigated erosion corrosion and found that aragonite, which is one polymorph of $CaCO_3$, particles of sizes < 2 mm are capable of creating leaks in copper pipes. Typically, the formation of large $CaCO_3$ particles is not a concern in potable water systems, however it has been shown that $CaCO_3$ scale can be removed from premise plumbing materials (copper and polypropylene) by shear stress (Royer et al., 2010). The scale that gets released has potential to cause or accelerate erosion corrosion, especially in recirculating systems.

The complexity of these phenomena and their profound impact on the infrastructure, energy and sustainable water nexus, make it an ideal time to revisit this important topic (Table 1-2). The objectives of this review are: (1) re-evaluate $CaCO_3$ formation in a modern context, such as global warming, autogenous repair, corrosion inhibitors and increasing water heater temperatures in building; (2) identify knowledge gaps regarding $CaCO_3$ formation and control.

Table 1-2: Recent phenomena and its effect on $CaCO_3$ formation

Phenomenon	Effects on $CaCO_3$ formation	Research priorities
Global warming	• Greater CO_2 in atmosphere can raise or lower amount of $CaCO_3$ that could form • More severe droughts could raise Ca^{2+} in natural waters	• Experimentally alter $CaCO_3$ formation potential at varying P_{CO2}
Corrosion and scaling inhibitors	• Phosphates added to drinking water reduce $CaCO_3$ formation • Use increased in last 25 years, but pressure on industry to lower the dosage for cost and environmental reasons • NOM is a scaling inhibitor, utilities are targeting it for removal because it is a precursor to DBPs	• Find out how $CaCO_3$ precipitation is affected by higher and lower phosphate concentrations • Effect of non-phosphate inhibitors on $CaCO_3$ precipitation
Raising water heater temperature	• Home and building owners are raising water heater temperatures to control opportunistic pathogens. Higher temperatures increase $CaCO_3$ scaling potential	• Improve water heater design to reach higher temperatures but reduce scaling potential
Autogenous repair	• $CaCO_3$ formation could beneficially be used to seal leaks in plumbing and distribution systems	• Alter chemistry of drinking water to promote leak repair via $CaCO_3$ • Examine the impact inhibitors have on ability to repair
Biofilm growth	• $CaCO_3$ provides a surface for biofilm to grow on. Shields biofilm from antimicrobial plumbing materials	• Determine health implications of $CaCO_3$-induced biofilm growth in domestic plumbing
Erosion corrosion	• Small (< 2 mm) $CaCO_3$ particles and $CaCO_3$ scale released from pipe surface can cause erosion corrosion	• Analyze flow patterns and plumbing design to mitigate erosion corrosion from $CaCO_3$

1.3 Chemistry of $CaCO_3$ Formation

1.3.1 Background

To fully understand practical aspects of $CaCO_3$ behavior in potable water systems, it is important to first review the chemistry of $CaCO_3$ formation and dissolution. $CaCO_3$ crystals are made up of Ca^{2+} and CO_3^{2-} lattice ions, both of which are ubiquitous in natural water systems. It can exist in three crystalline polymorphs as well as an amorphous phase (ACC) or as a mono- and hexahydrate. The solubility product for each form varies with temperature (Table 1-3). $CaCO_3$ has significantly lower solubility at higher temperatures, causing $CaCO_3$ formation to be a major issue in many hot water systems even when it is not a problem in cold water systems for waters with moderate hardness and alkalinity (Figure 1-3).

Table 1-3: Temperature dependence of solubility product for $CaCO_3$ polymorphs

Polymorph	pK_{sp} at 25 °C	K_{sp} Equation	Temperature Range	References
ACC	6.04	$\log K_{sp} = \frac{1247}{T} - 10.224$	16 to 60 °C	Clarkson et al., 1992
Vaterite	7.91	$\log K_{sp} = -172.1295 - 0.077993 * T + \frac{3074.688}{T} + 71.595 * \log T$	0 to 90 °C	Plummer and Busenberg, 1982
Aragonite	8.34	$\log K_{sp} = -171.9773 - 0.077993 * T + \frac{2903.293}{T} + 71.595 * \log T$	0 to 90 °C	Plummer and Busenberg, 1982
Calcite	8.48	$\log K_{sp} = -171.9065 - 0.077993 * T + \frac{2839.319}{T} + 71.595 * \log T$	0 to 90 °C	Plummer and Busenberg, 1982

Note: T is temperature in K.

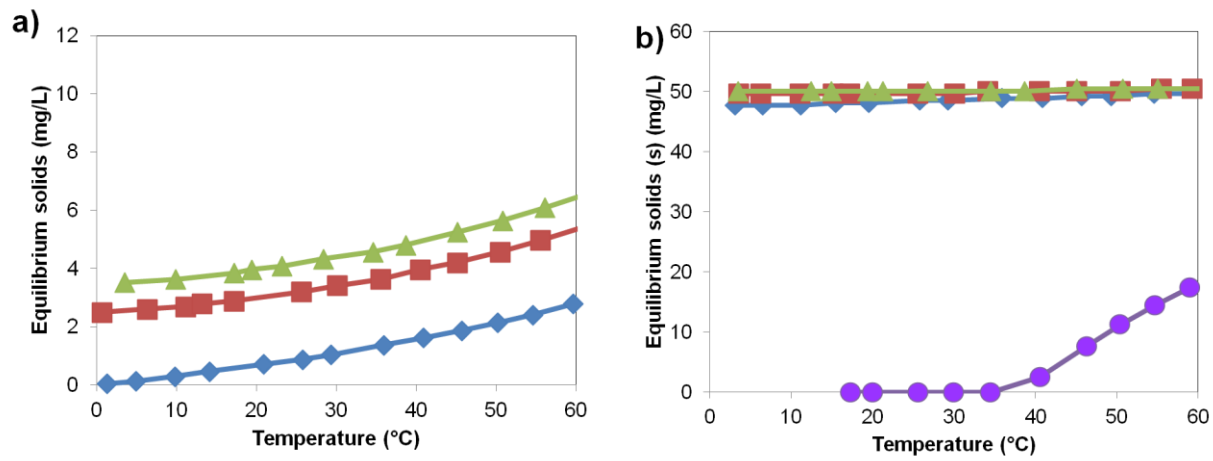

Figure 1-3 Impact of increasing temperature on $CaCO_3$ formation: The amount of potential $CaCO_3$ formation for all crystalline polymorphs (vaterite, aragonite and calcite) and ACC under different temperatures in water distribution systems. MINEQL+ simulations on a closed system with alkalinity = 100 mg/L as $CaCO_3$ at pH 8.5 and (a) initial TOTCa = 40 mg/L and (b) initial TOTCa= 65 mg/L.

While the levels of Ca^{2+} in natural waters are usually governed by regional geology (limestone, dolomite, etc.), the carbonate system is more complex. The pK_a values indicate that CO_3^{2-} becomes the dominant form of inorganic carbon at pH 10.3 and higher (Plummer and Busenberg, 1982).

$$CO_2(g) + H_2O \rightleftharpoons CO_2(aq) + H_2CO_3(aq) \qquad pK_H = 1.47$$
$$H_2CO_3(aq) \rightleftharpoons H^+ + HCO_3^-(aq) \qquad pK_{a1} = 6.4$$
$$HCO_3^-(aq) \rightleftharpoons H^+ + CO_3^{2-}(aq) \qquad pK_{a2} = 10.3$$

The ion activity product, Q, for $CaCO_3$ is the product of the Ca^{2+} and CO_3^{2-} activities as shown in the equation below.

$$Q = \{Ca^{2+}\}\{CO_3^{2-}\}$$

When $Q < K_{sp}$, the solution is undersaturated, precipitation is not thermodynamically favored, and solid $CaCO_3$ can dissolve. However, when $Q > K_{sp}$, $CaCO_3$ is supersaturated and can precipitate.

Precipitation starts with nucleation, which is the initiation of phase change from aqueous to solid in the solution. Nucleation is categorized as primary and secondary. Primary nucleation refers to nucleation when no other crystals are present (Mullin, 2001). It can occur homogeneously (spontaneous and in the absence of any solids) or heterogeneously (nucleation induced by foreign solid particles). Heterogeneous nucleation is more commonly observed for $CaCO_3$ because the surface of the foreign solid generally lowers the activation energy barrier for nucleation (Brezonik and Arnold, 2011). Secondary nucleation refers to the growth of $CaCO_3$ on pre-existing crystals (Mullin, 2001).

The induction time, τ, is defined as the time between the moment the solution reaches supersaturation and the onset of precipitation. A general model for induction time for $CaCO_3$ precipitation is given by Xyla et al. (1991) as

$$\tau = K(\Omega^{0.5} - 1)^p$$

Where K depends on the system's characteristics, p is apparent growth order (for $CaCO_3$, p was determined to be 8.0 [Xyla et al., 1991]), and Ω is the degree of supersaturation, defined as

$$\Omega = \frac{Q}{K_{sp}}$$

Typical induction times for homogeneous precipitation can range from <1 to 136 minutes depending on Ω and assuming there are no impurities (i.e. inhibitors) (Xyla et al. 1991).

1.3.2 Precipitation and Growth in Plumbing and Distribution Systems

Homogeneous Precipitation

Homogeneous nucleation of $CaCO_3$ occurs less frequently than heterogeneous nucleation due to the larger energy barrier of spontaneously forming $CaCO_3$ nuclei in solution. As a result, homogeneous nucleation is mostly observed at Ω greater than 1.6 (Lioliou et al., 2007).

Homogeneous nucleation of $CaCO_3$ was believed to follow classical nucleation theory (CNT). CNT states that a nucleus is not stabilized until a critical radius is reached in which the bulk energy and surface energy of the nuclei is balanced (Gebauer et al., 2014). However, the recent discovery of pre-nucleation clusters (PNCs) undermines CNT (Gebauer et al., 2008). PNCs contain $CaCO_3$ lattice ions but do not have an explicit phase boundary with the solution. There are also structural characteristics of PNCs that indicate which polymorph nucleates. More stable PNCs yield ACC with short-range order corresponding to calcite while less stable PNCs yield ACC with short-range order corresponding to vaterite (Lam et al., 2007; Gebauer et al., 2014).

Homogeneous $CaCO_3$ precipitation roughly follows Ostwald's rule of stages. The rule of stages states that often the least stable polymorph crystallizes first before transforming into the most stable polymorph (Ng et al., 1996). For $CaCO_3$, ACC is the first to precipitate, followed by vaterite, before transforming into calcite which is its most stable form (Wolf et al., 2008). Ogino et al. (1987) observed the same at lower temperatures (14-30 °C) while at higher temperatures (60-80 °C), the transition of ACC to aragonite to calcite was observed. At intermediate temperatures (40-50 °C), $CaCO_3$ crystallization closely follows Ostwald's rule of stages because every polymorph forms before becoming calcite (Ogino et al., 1987).

$CaCO_3$ scale that forms in plumbing and distribution systems is unlikely to have originated from homogeneous nucleation. The large energy barrier for homogeneous nucleation means the solution must have a higher Ω for $CaCO_3$ to readily precipitate. Even in systems that stagnate for long periods of time, heterogeneous nucleation is likely to be the more common form of nucleation due to the scale already present or bare surfaces that lower the energy barrier for nucleation.

Heterogeneous Precipitation

As discussed previously, heterogeneous nucleation occurs more readily than homogeneous nucleation due to the lower energy barrier the surface provides. As a result, it is likely the most common route of nucleation for $CaCO_3$ scale in plumbing and distribution systems.

Many characteristics of surface materials will affect heterogeneous precipitation of $CaCO_3$, such as surface roughness (Keysar et al., 1994; Wu et al., 2010; Cheong et al., 2013; MacAdam and

Parsons, 2004a) and surface charge (Wu et al., 2010). Several studies have been conducted to determine the susceptibility of $CaCO_3$ to scale surfaces made of different materials. In general, inert materials such as polymers are less likely to scale than metallic surfaces (Githens et al., 1965). In a study done on heated metallic surfaces, it was found that copper has the highest scaling rate compared to steel and aluminum (Macadam and Parsons, 2004a). These results contradict those of a previous experiment that observed aluminum as having the highest scaling rate followed by mild steel, then copper (Troup and Richardson, 1978).

Comparing copper and polypropylene tubes in heat exchangers, copper was scaled with Ca-containing minerals at a rate twice that of polypropylene (Wu et al., 2009). However, a similar study found no significant difference between $CaCO_3$ scaling on copper and polymer surface including polypropylene (Wang et al., 2005). Comparison of heterogeneous nucleation on PVC and stainless steel surfaces shows that stainless steel has higher precipitation rate at low Ca^{2+} concentration (200 mg/L as $CaCO_3$), however at higher Ca^{2+} concentration (400 mg/L as $CaCO_3$) higher heterogeneous precipitation rate was observed on PVC (Amor et al., 2004). There is a gap in research comparing the heterogeneous nucleation on traditional water distribution system materials (i.e. concrete and cast iron). Predictions about the heterogeneous nucleation rate can be made using absolute surface roughness. The Hazen-Williams coefficient (C-factor) for concrete is 100 and for cast iron is 80-130, depending on age (Jaćimović et al., 2015). Lower C-factors indicate a rougher surface; thus aged cast iron would have a higher scaling potential than concrete.

It is also important to consider $CaCO_3$ nucleation on waterborne particles because bulk precipitation can enhance scaling (Andritsos and Karabelas, 2003; Pääkkönen et al., 2009). Although suspended calcite crystals are the most effective $CaCO_3$ seeds (Nancollas and Reddy, 1971; Lin and Singer, 2005b), they are relatively uncommon in natural waters. Some particles that make up clay, which contributes to turbidity, have shown to induce $CaCO_3$ precipitation. For example, montmorillonite, a type of clay, was shown to instantaneously lead to calcite precipitation (Kralj and Vdović, 2000).

Surface free energy is believed to influence heterogeneous $CaCO_3$ nucleation. Lower surface energy reduces the adhesion strength of $CaCO_3$ (Müller-Steinhagen and Zhao, 1997; Förster et al.,

1999; Yang et al., 2000; Yang et al., 2002; MacAdam and Parsons, 2004b). Müller-Steinhagen and Zhao (1997) successfully reduced $CaSO_4$ scaling rate on stainless steel by lowering its surface energy via ion implantation. Förster et al. (1999) also found a negative correlation between surface energy and induction time for $CaSO_4$ formation on a variety of materials. A similar result might be expected with $CaCO_3$.

Growth Rate

Previous models of seeded growth kinetics only considered Ω. Morse (1983) modeled the growth rate using the equation below.

$$R = k(\Omega - 1)^n$$

Where R is the rate of precipitation normalized to surface area, k is an empirical rate constant, and n is reaction order. The general growth rate of $CaCO_3$ has also been modeled in terms of the rate of decrease in Ca^{2+} concentration as shown in the equation below (Kazmierczak et al., 1982; Nancollas and Reddy, 1971).

$$-\frac{d[Ca^{2+}]}{dt} = ks([\{Ca^{2+}\}\{CO_3^{2-}\}]^{0.5} - K_{so}^{0.5})^2$$

Where k is the rate constant for growth and s is a function of the crystal surface area. The two growth models shown so far only consider the degree of supersaturation. Lin and Singer (2005b) did extensive research on the surface reactions occurring during $CaCO_3$ growth and found positive correlation between $CaCO_3^0$ with the surface species $>CaCO_3^-$ and $>CO_3^-$.

For $CaCO_3$ crystallization, the growth mechanism can be either surface-controlled or diffusion-controlled. In a surface-controlled mechanism, incorporation of lattice ions into the crystal structure is the rate limiting process. In a diffusion-controlled mechanism, diffusion of lattice ions from the solution to the crystal surface is the rate limiting process. Past research points toward the surface-controlled mechanism being dominant in $CaCO_3$ crystallization (Rodriguez-Hornedo and Murphy, 1999; Xyla et al., 1991; Dalas et al., 1988; Lioliou et al., 2007). However, pH,

supersaturation, and hydrodynamic conditions can influence whether the rate is surface- or diffusion-controlled (Lin and Singer, 2005b).

Dissolution

Numerous comprehensive studies on calcite dissolution kinetics or the dissolution of carbonate minerals in general determined that dissolution occurs by the following mechanism (Berner and Morse, 1974; Plummer et al., 1978; Chou et al., 1989).

$$CaCO_3 + H^+ \rightleftharpoons Ca^{2+} + HCO_3^-$$
$$CaCO_3 + H_2CO_3^* \rightleftharpoons Ca^{2+} + 2HCO_3^-$$
$$CaCO_3 + H_2O \rightleftharpoons Ca^{2+} + HCO_3^- + OH^-$$

The first mechanism has a first-order dependence on H^+ activity and is the most affected by changes in pH (k_1). The second mechanism describes a first-order dependence on CO_2 (aq) and H_2CO_3 and therefore has a linear dependence on P_{CO2} (k_2). However, dissolution is nearly independent from P_{CO2} at low levels such as those found in the atmosphere (Plummer et al., 1978). The third mechanism describes dissolution at low H^+ activity and dissolved CO_2 (k_3). For the final rate expression, given in the equation below, there is an additional term for calcite precipitation whose rate constant, k_4, is a function of temperature and P_{CO2} (Plummer et al., 1978; Reddy et al., 1981).

$$R = k_1\{H^+\} + k_2\{H_2CO_3^*\} + k_3\{H_2O\} - k_4\{Ca^{2+}\}\{HCO_3^-\}$$

Rate constants depend on the pH of the system and transport of ions, however dissolution via the first mechanism is the largest contributor to dissolution and this mechanism is often diffusion-controlled (Berner and Morse, 1974; Plummer et al., 1978).

1.3.3 Morphology and Polymorph Stability

Although calcite is the thermodynamically stable polymorph in most cases, solution temperature can impact the stability and metastability of aragonite and vaterite. At temperatures greater than

60 °C, homogeneous precipitation yields aragonite as the dominant polymorph over a period of hours (Wray and Daniels, 1957; Sawada, 1997; Kellermeier et al., 2013). Temperature also affects the relative abundance of each polymorph during the early metastable stage of homogeneous precipitation. Vaterite is the dominant metastable phase at standard temperature, however at temperatures below 25 °C, calcite is the dominant metastable phase and at temperatures above 50 °C, aragonite is the dominant metastable phase (Ogino et al., 1987).

The mechanism of $CaCO_3$ precipitation and calcite formation occurs in stages via redissolution of ACC to vaterite and vaterite to calcite over a period of approximately 3 hours (Ogino et al., 1987; Sawada, 1997). Knowing the polymorph evolution as $CaCO_3$ precipitates could have importance in predicting scale formation. Some sources reference formation of "hard" calcite scale and "soft" aragonite scale that is easier to be removed (Liu et al., 2010). Although this claim is unverified, if it is true, the time between $CaCO_3$ precipitation and "hard" scale deposition could be predicted in some systems.

1.4 Monitoring $CaCO_3$ Formation in Potable Water Systems

1.4.1 Tests and Indices for Scale Formation

The problems caused by scaling have led to the development of numerous scaling indices (Table 1-4) to monitor $CaCO_3$ formation in potable water systems. Degree of supersaturation (Ω) is the most widely accepted scaling index, however, it only accounts for chemical equilibrium in determining whether scaling will occur, and does not account for reaction kinetics. As discussed in the previous sections, $CaCO_3$ precipitation and dissolution can occur very slowly, especially in the presence of natural and artificial scaling inhibitors—thus calculation of Ω is only a first step to predicting scaling in potable water systems. The only measure that takes into account actual precipitation kinetics is temporary hardness. Temporary hardness represents the amount of hardness that precipitates by boiling water, and was once widely applied as a practical way of describing scaling potential of water heating systems. In practice, temporary hardness does not often differentiate the precipitated solids so it is not only a measure of $CaCO_3$ precipitation but also of $MgCO_3$ and sulfate salts (Greth, 1910; Buswell, 1916; Goudey, 1933). Temporary hardness has also been defined strictly as carbonate hardness which in the past was measured by titration

and soap tests (Hehner, 1883; Norton and Knowles, 1916). Despite its simplicity, the temporary hardness test could still have value as a quick test for scaling potential.

Table 1-4: Scaling indices used in practice

Index or test	Definition	Scaling condition	Accounts for Kinetics?
Degree of supersaturation	$\Omega = \frac{\{Ca^{2+}\}\{CO_3^{2-}\}}{K_{sp}}$	$\Omega > 1$	No
Langelier saturation index (LSI)	$LSI = pH_{actual} - pH_{saturated}$ where $pH_{saturated} = pK_2 - pK_s + pCa + pAlk$	$LSI > 0$	No
Ryznar stability index (RI)	$RSI = 2 \cdot pH_{saturated} - pH_{actual}$	$RSI < 6.2$	No
Puckorius scaling index (PSI)	$PSI = 2 \cdot pH_{saturated} - pH_{equilibrium}$ where $pH_{equilibrium} = 1.47 + \log(Alk) + 4.54$	$PSI < 6$	No
Larson-Skold index (LI)	$LI = [(Cl^-) + (SO_4^{2-})]/[(HCO_3^-) + (CO_3^{2-})]$	$LI < 0.8$	No
Calcium carbonate precipitation potential (CCPP)	$CCPP = 50{,}000([Alk]-[Alk]_{equilibrium})$ For $[Alk]_{equilibrium}$ calculation, refer to U.S. EPA, 1992	CCPP > 4 mg/L	No
Aggressive Index (AI)	$AI = pH + \log([Alk] \cdot [Hardness])$, where [Alk] and [Hardness] are in mg/L as $CaCO_3$	$AI > 12$	No
Temporary hardness	Water is heated until no more minerals precipitate, standard method is unknown	Measured by hardness loss	Yes

There are several more indices that aim to predict scaling in specific systems. The Langelier saturation index (LSI) was first described in Langelier (1936) as a way to predict the formation of a corrosion-resistant $CaCO_3$ coating in distribution systems and has since been revised (Wojtowicz, 2001). LSI has been called an oversimplification in that it assumes pH and $CaCO_3$ saturation are the most important factors for corrosion control (Schneider and Stumm, 1964) and it does not account for other dissolved calcium species or other forms of alkalinity (Kutty et al., 1992). Dabrowski et al. (2010) tested the LSI on a water distribution system and found no correlation between waters with LSI < 0 and a water's aggressiveness.

Indices developed after LSI are similar to LSI in that they express $CaCO_3$ undersaturation or supersaturation, but take into account and emphasize different factors such as equilibrium pH and non-carbonate hardness. The Ryznar stability index (RI) still uses $pH_{saturated}$ like the LSI, however, it recognizes calcium and alkalinity as more important parameters in determining scale formation potential, thus $pH_{saturated}$ is multiplied by a factor of 2 (Ryznar and Langelier, 1944). The RI was successfully tested on real waters where it was determined that an RI < 6.2 should form scale. The Puckorius scaling index (PSI) was formulated for cooling tower water and includes a term for $pH_{equilibrium}$, which depends on alkalinity (Puckorius and Brooke, 1991). PSI stresses the importance of alkalinity in scale formation, because a higher alkalinity increases the water's buffering capacity such that more $CaCO_3$ is able to precipitate before the water reaches equilibrium pH. Unlike the other indices, the Larson-Skold index (LI) does not use $pH_{saturated}$ in its calculation. LI was originally intended for Great Lakes waters traveling through steel distribution lines (Larson and Skold, 1958) and is best suited for waters of similar quality. LI considers the effect of Cl^- and SO_4^{2-} on $CaCO_3$ film formation, since higher Cl^- and SO_4^{2-} levels usually indicate a greater presence of non-carbonate hardness (e.g. $CaSO_4$), which is not conducive to scale formation in potable water systems.

The aggressive index (AI) was developed to monitor the corrosiveness of water in asbestos cement pipes. AI < 10 indicates a highly aggressive (corrosive) water and AI > 12 indicates a nonaggressive water (NRC, 1982). Due to the AI's simplicity, it could be considered one of the weaker scaling indices, as it does not account for temperature or ionic strength like the other indices do.

The calcium carbonate precipitation potential (CCPP) is unique in that it attempts to quantify the amount of $CaCO_3$ that could precipitate. For the purpose of corrosion control, the EPA once recommended that the CCPP should have a value of 4 - 10 mg/L to form a thin protective coating (U.S. EPA, 1992). CCPP relies on the estimation of the equilibrium alkalinity, $[Alk]_{equilibrium}$, through an iterative process. Rossum and Merrill's (1983) study comparing several scaling indices found that CCPP is the best estimate of a water's ability to deposit or dissolve $CaCO_3$.

1.4.2 In-Situ Monitoring of Scale

Several in-situ methods have been used to monitor scale formation. These methods are often used in experiments for the purpose of optimizing anti-scaling techniques. For water heating systems, scale can be monitored by measuring changes in the overall heat transfer coefficient. Al-Deffeeri (2007) implemented this method on a multi-stage flash distillation desalination process to optimize it.

The use of focused beam reflection measurement (FBRM) has also proven capable of monitoring scale formation (Al Nasser et al., 2008; Al Nasser et al., 2011). Instead of measuring the mass of the deposited scale, the number of crystals deposited over the FBRM probe is measured as well as the size distribution of these crystals.

Neville et al. (1999) tested the rotating disk electrode (RDE) method on detecting $CaCO_3$ scale. RDE is based on the oxygen reduction reaction; as scale accumulates over the RDE, less of the surface is exposed to the bulk solution and the rate of oxygen reduction is slowed. One of the benefits of RDE is that it is applicable to many waters of different quality and flow conditions.

1.5 Control and prevention of calcium carbonate scaling

To control and prevent $CaCO_3$ scaling issues, the first and foremost step is to monitor the scaling potential of drinking water (e.g. degree of supersaturation, Langelier saturation index) at different points of the distribution system as discussed in Section 4. Once $CaCO_3$ scaling potential is

confirmed, different control and prevention methods might be applied for specific environmental conditions and water compositions (Table 1-5).

Table 1-5: Control and prevention of $CaCO_3$ scaling in drinking water systems

Methods	Likely effects	Rationale
Control $CaCO_3$ precipitation		
Decrease hot water temperature	Effective	Solubility products of $CaCO_3$ increase with decreasing water temperature.
Decrease water pH	Effective	Saturation ratios of $CaCO_3$ decrease with decreasing pH.
Remove dissolved Ca	Effective	Saturation ratios of $CaCO_3$ decrease with decreasing dissolved Ca concentration.
Control $CaCO_3$ morphology	Sometimes effective	Reduce scaling potential, by preferring the $CaCO_3$ polymorph with a higher solubility product to form first.
Control the use of surface materials	Sometimes effective	Scaling potentials of $CaCO_3$ are different on various surface materials.
Control the location of $CaCO_3$ formation	Sometimes effective	Phosphates delay the formation of $CaCO_3$, so that it occurs throughout potable water systems.
Delay or prevent $CaCO_3$ precipitation		
Scale inhibitors	Effective	Delay or prevent $CaCO_3$ precipitation completely, mostly by adsorption of inhibitors onto $CaCO_3$ nuclei.
Potential beneficial application of $CaCO_3$		
Control $CaCO_3$ precipitation for autogenous repair of pipe leaks	N/A	Precipitation of $CaCO_3$ is allowed. However, the precipitated $CaCO_3$ particles can be used for autogenous repair of the leaks in drinking water pipelines. (Tang et al., 2013)
Dutch pellet softening method	Effective	Precipitation of $CaCO_3$ on calcite pellets removes supersaturation when water passes through a column of calcite pellets. Contact time and surface area are important parameters. (Schetters, 2013)

1.5.1 Controlling $CaCO_3$ precipitation through water chemistry parameters

Temperature

Reducing water temperature is very effective in reducing $CaCO_3$ scaling potential in potable water systems. First, the solubility of all $CaCO_3$ polymorphs (calcite, vaterite, aragonite, and amorphous $CaCO_3$) increase with decreasing temperature (Clarkson et al., 1992; Plummer and Busenberg, 1982), causing less $CaCO_3$ to precipitate at lower temperature. Second, the reaction kinetics for $CaCO_3$ formation is much slower at lower temperatures (Morse et al., 2007), thereby forming less

$CaCO_3$ precipitates. Finally, polyphosphates, which are widely present in potable water systems and are stronger inhibitors for $CaCO_3$ precipitation than orthophosphate (Lin and Singer, 2005), are converted into orthophosphate much faster at higher temperature through hydrolysis reactions (Holm and Edwards, 2003). Hence, at a lower temperature, more polyphosphates are present and will inhibit $CaCO_3$ precipitation more. However, the temperature drop for hot water might cause Opportunistic Premise Plumbing Pathogens (OPPPs), including *Legionella pneumophila*, to grow and transmit in drinking water systems and cause potential human health problems (ASHRAE, 2015).

To further illustrate how effective reducing water temperature is in controlling $CaCO_3$ precipitation, we compared the scaling potentials of all the potable water samples collected from a national survey at different temperatures relevant to potable water systems (Figure 1-4) (U.S. EPA, 2000). In our calculation, we chose calcite saturation ratio ($\Omega_{calcite}$) to represent the calcite scaling potentials for the 51,846 water samples collected from water utilities in the U.S., and we only accounted for solubility change at different temperatures. As water temperature increased from ambient temperature to higher temperatures, the percentage of water samples that are at risk of scaling ($\Omega_{calcite} > 1$) is 59% (or 30,538 water samples) at 48 °C and 62% (or 31,910) at 60 °C, which is much higher than the 47% (or 24,468 water samples) at the ambient temperature (Figure 1-4b). This clearly indicates that more waters are at higher scaling risks as temperature increases, due to the decreasing calcite solubility. In addition, most of these water samples do not have very high Ca hardness (soft and moderately hard), which might explain why most of these water samples do not have high scaling potentials at ambient temperatures (Figure 1-4c).

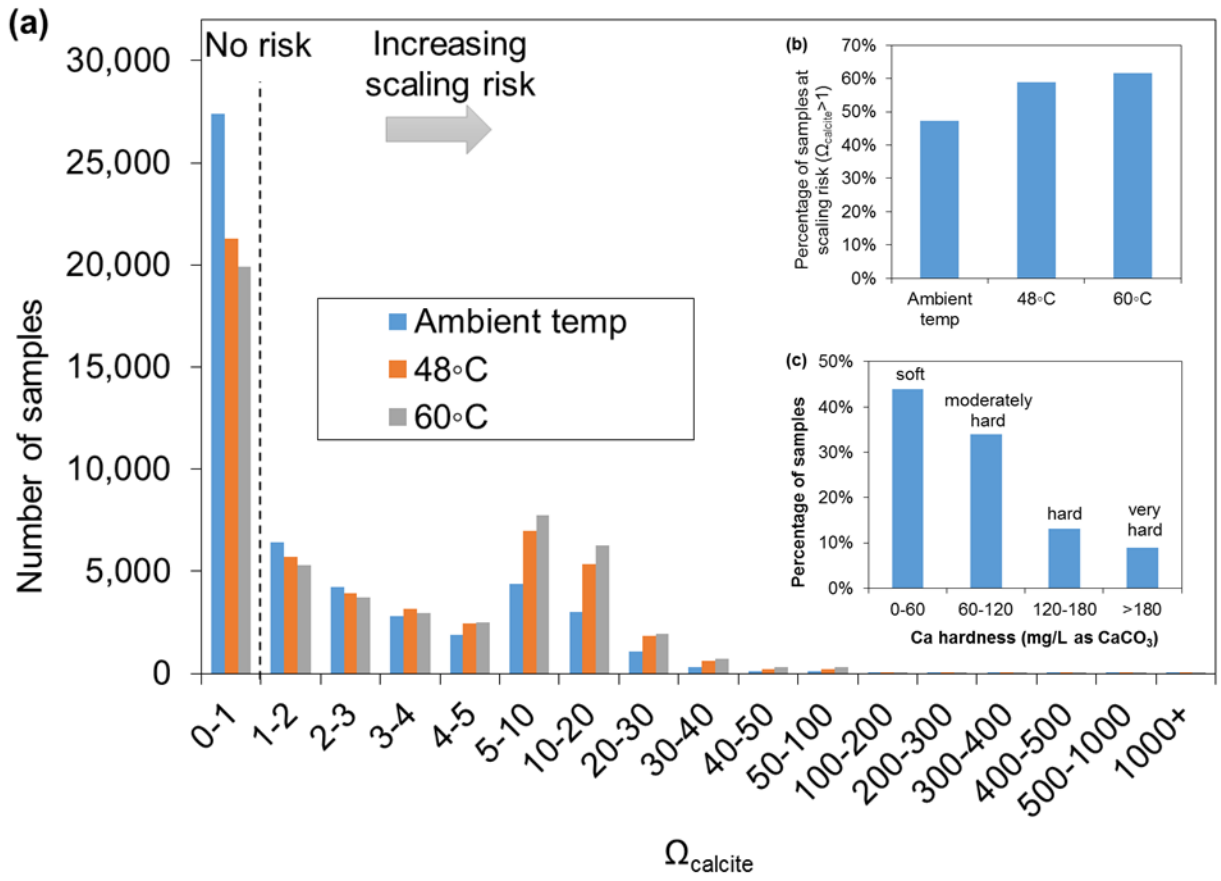

Figure 1-4 Scaling potential in potable water systems throughout the U.S.: The scaling potentials of water samples collected from a national survey at different temperatures relevant to potable water systems (U.S. EPA, 2000). (a) Histogram of saturation ratio of calcite ($\Omega_{calcite}$) at various temperatures, (b) the percentage of water samples at scaling risks ($\Omega_{calcite}$ >1), and (c) the percentage of water samples at different Ca hardness levels. The saturation ratio of calcite was calculated for 48 ºC and 60 ºC, in addition to the ambient temperature provided in the national survey (U.S. EPA, 2000). MATLAB was used to calculate $\Omega_{calcite}$ for 51,846 water samples that have all four parameters of temperature, pH, alkalinity, and Ca hardness. The change of equilibrium constants (K) and solubility products (K_{sp}) with temperature was accounted for using the K and K_{sp} values and ΔH at 25 ºC from MINEQL+. Ca-containing species considered included Ca^{2+}, $CaHCO_3^+$, $CaOH^+$, and $CaCO_{3(aq)}$.

Water pH

Reducing water pH and removing dissolved Ca content can reduce scaling potential by decreasing the ion activity product ($Q = \{Ca^{2+}\}\{CO_3^{2-}\}$). However, engineers should be careful when considering reducing water pH in drinking water systems, because the decrease in water pH might cause corrosion of metallic pipelines.

1.5.2 Other methods that might be effective in controlling $CaCO_3$ scaling

Stabilization of metastable $CaCO_3$ polymorphs over calcite by including different additives might be effective in controlling $CaCO_3$ scaling potential. Additives, including metal cations, silica and organic species, can help stabilize metastable $CaCO_3$ polymorphs, such as aragonite, vaterite and ACC (Table 1-6). Zn^{2+} is the only additive that has been reported to help avoid massive calcite scaling when dosed at a concentration relevant to drinking water (1.5×10^{-7} - 1.5×10^{-4} M), by preferring aragonite nuclei to form instead of calcite. As a result, Zn can co-precipitate into aragonite nuclei or adsorb on aragonite nuclei and inhibit the further growth of $CaCO_3$ crystals (Wada et al., 1995; Ghizellaoui and Euvrard, 2008). Other additives must be dosed at concentrations that are much higher than their typical concentrations in drinking water. For example, when silica is added at a concentration of 3.3×10^{-3} - 0.2 M, metastable $CaCO_3$ polymorphs can be stabilized to co-exist with calcite for as long as 2 hours at 50 ^{o}C and 80 ^{o}C (Kellermeier et al., 2013).

Table 1-6: Different additives and their favored $CaCO_3$ polymorphs

	Species	Concentration	Favored $CaCO_3$ polymorph	References
Cations	Fe^{2+}, Mg^{2+}, Ni^{2+} Co^{2+}, Cu^{2+}	0.2 - 3.0 M	Aragonite	Wada et al., 1995
	Zn^{2+}	1.5×10^{-7} - 1.5×10^{-4} M	Aragonite	Wada et al., 1995; Ghizellaoui and Euvrard., 2008
Silica	SiO_2	3.3×10^{-3} - 0.2 M	vaterite, aragonite, and ACC	Kellermeier et al., 2013
Organic	PAA, PBTCA	5 - 25 mg/L	vaterite, aragonite	Yang et al., 2001
	OMM	8 - 20 mg/L	Vaterite	Roque et al., 2004

Note: PAA is the abbreviation of polyacrylic acid, PBTCA is the abbreviation of is 2-phosphonobutane-1,2,4-tricarboxylic acid, and OMM is the abbreviation of organic matrix macromolecules.

Surface materials and roughness might affect $CaCO_3$ scaling potentials as well as the physical and mechanical properties of scales. Since $CaCO_3$ can form through heterogeneous nucleation on different surface materials, the surface energy and the nucleation energy barrier of different surface materials will affect $CaCO_3$ scaling potentials. As discussed in section 3.2.2, copper surface has a lower scaling potential than polypropylene (Wu et al., 2010), while stainless steel and aluminum surfaces have similar scaling potentials (Dalas and Koutsoukos, 1990). In addition, the roughness of the surface materials can affect the physical and mechanical properties of $CaCO_3$ scales (e.g. porosity and tensile strength). For mild steel surfaces, the rougher the surfaces, the lower porosity and higher tensile strength the $CaCO_3$ scales possess (Keysar et al., 1994). This might be due to enhanced surface nucleation density and a certain orientation of the calcite structure.

1.5.3 Delay or prevent $CaCO_3$ precipitation using scale inhibitors

Scale inhibitors can effectively delay or even completely prevent $CaCO_3$ scaling problems. Scale inhibitors are widely used to combat severe scaling issues in water processing equipment that handle large volumes of water, including cooling towers and production wells in oil and gas fields.

These scale inhibitors generally include phosphonates, phosphate esters, polyacrylates and phosphates (Matty and Tomson, 1988; Shakkthivel and Vasudevan, 2006; Xyla et al., 1992). However, most of these inhibitors are not used in drinking water systems (except polyphosphates or phosphates).

Inorganic cations Mg^{2+} and Zn^{2+} that are readily present in drinking water systems can act as scale inhibitors (Table 1-7). Addition of Mg^{2+} at a concentration of 10^{-3} M and above can significantly inhibit calcite precipitation (Reddy and Wang, 1980; Lin and Singer, 2009). The mechanism behind the inhibiting effect of Mg^{2+} has been confirmed as the adsorption of Mg^{2+} onto calcite active crystal growth sites (or kinks) and subsequent kink blocking (Lin and Singer, 2009; Nielsen et al., 2013), rather than the previously proposed mechanisms of increasing the mineral solubility by incorporating Mg^{2+} into calcite (or incorporation inhibition) (Davis et al., 2000). Addition of Zn^{2+} at a much smaller concentration (~10^{-7} M) can also significantly inhibit calcite precipitation (Ghizellaoui and Euvrard, 2008). It is possible Zn^{2+} can inhibit $CaCO_3$ (calcite or aragonite) precipitation through either kink blocking or incorporation inhibition, but the exact mechanism behind this inhibiting effect by Zn^{2+} has not yet been identified. However, no threshold values can be identified for either Mg^{2+} or Zn^{2+}, because they reduce the $CaCO_3$ precipitation rate even at very low concentrations, rather than abruptly halt calcite precipitation once a threshold value is reached.

Other organic inhibitors that widely exist in drinking water systems are phosphates and natural organic matter (or NOM) (Table 1-7). Lin and Singer systematically studied the inhibiting effects of orthophosphate (PO_4^{3-}), pyrophosphate ($P_2O_7^{4-}$), tripolyphosphate ($P_3O_{10}^{5-}$), hexametaphosphate ($P_6O_{18}^{6-}$) and binary-polyphosphate blends, and suggested that a total P concentration of 10^{-8} M and above can inhibit calcite precipitation (Lin and Singer, 2006; Lin and Singer, 2005a). The reason for this inhibiting effect is the adsorption of phosphates onto calcite crystal growth sites and blocking further growth. NOM, such as fulvic acid and humic acid, can also inhibit calcite precipitation through a similar mechanism to phosphates (Lin et al., 2005; Hoch et al., 2000).

Table 1-7: Effective concentrations of $CaCO_3$ scale inhibitors in drinking water systems

Scale inhibitors		Effective concentration	References
Inorganic inhibitors	Mg^{2+}	6 ~ 21 ($\times 10^{-3}$ M)	Lin and Singer, 2009
	Zn^{2+}	2 ~7 ($\times 10^{-7}$ M)	Ghizellaoui and Euvrard, 2008
Organic inhibitors	Phosphates [1]	1 ~ 5 ($\times 10^{-8}$ M)	Lin and Singer, 2005a
			Lin and Singer, 2006
	NOM [2]	1 ~ 5 (mg/L)	Lin et al., 2005

[1] Phosphates include orthophosphate, pyrophosphate, tripolyphosphate and hexametaphosphate.

[2] NOM includes Suwannee River fulvic acid, Pacific Ocean fulvic acid, and Williams Lake hydrophobic organic acid.

Phosphates can be used to advantageously control the location of $CaCO_3$ formation in potable water systems. Addition of excess lime may only tend to coat the pipeline near the point of addition (Hatch, 1942). However, addition of orthophosphate (Hatch, 1942) and polyphosphate (Hasson and Karmon, 1981; McCauley, 1960), including hexametaphosphate (Primus and Hunhoff, 1972), to supersaturated waters could delay precipitation or prevent it completely, potentially extending the distance that pipes are coated from $CaCO_3$ formation.

1.5.4 Potential beneficial application of $CaCO_3$ precipitation for autogenous repair

Although usually considered harmful, $CaCO_3$ precipitation might be potentially beneficial when manipulated to repair leaks in drinking water systems via autogenous repair (i.e., leak self-repair) (Edvardsen, 1999; Clear, 1985; Tang et al., 2013). Autogenous repair is a promising and low cost approach to leak repair that can be achieved by manipulating the water chemistry and formation of $CaCO_3$ (e.g., calcite) to clog small leaks (holes typically $\approx$ 10 μm diameter) (Tang et al., 2013). If successfully applied, autogenous repair through $CaCO_3$ precipitation might help stop water losses that cost about $3 billion per year (FHWA, 2002), and extend the lifetime of the critically important and aging drinking water infrastructure that is expected to cost at least $1 trillion to repair, replace and upgrade through 2035, according to an estimate by the American Water Works Association (AWWA) (Shanaghan, 2012).

The possible mechanisms of autogenous repair by $CaCO_3$ precipitation are either the formation of precipitates directly in leaks (smart precipitation) or the clogging of the leaks when precipitates pass through the leaks (physical clogging) (Figure 1-5) (Tang et al., 2013). It is even possible that these two mechanisms may be operative simultaneously.

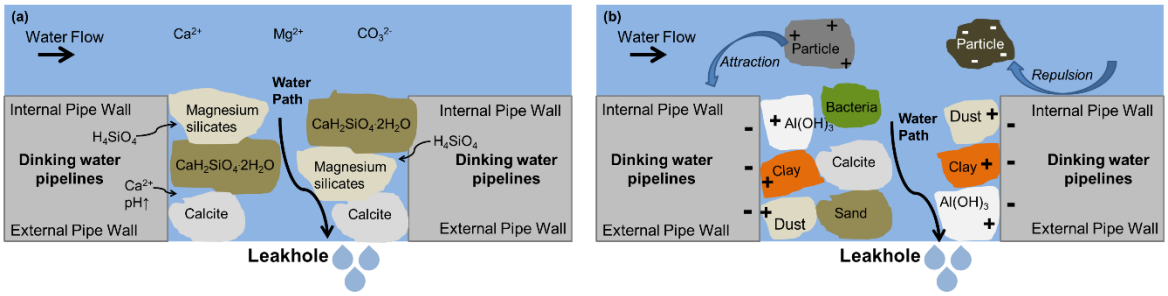

Figure 1-5 Autogenous repair of leaks by $CaCO_3$ precipitation in drinking water pipelines: **(**a) smart precipitation and (b) physical clogging. (Adopted from Tang et al., 2013)

One potential problem of autogenous repair or clogging by $CaCO_3$ precipitation is the long-term resistance to dissolution and longevity of the repair. It is possible that the repair materials (i.e. $CaCO_3$) might start to dissolve, once a water that is undersaturated with respect to $CaCO_3$ is pumped through the drinking water pipelines. However, since $CaCO_3$ dissolution is not very fast at pH $\geq$ 5 (Morse and Arvidson, 2002) and ambient temperature, the repair might be relatively long-lived, even when the water is relatively undersaturated.

1.5.5 Combating scaling by homeowners

Various water treatment devices have become commercially available for homeowners to combat scaling issues (Table 1-8), and most of them have a strong scientific basis. First, ion exchange softeners are designed to exchange Ca^{2+} with Na^{+}, reducing the dissolved Ca^{2+} concentration and scaling potentials in drinking water. Second, membrane treatments (nanofilters and reverse osmosis) can remove dissolved Ca^{2+} and inorganic carbon to reduce scaling potential, without introducing net extra salinity into the drinking water systems considering both reject water and treated water streams. Third, surface catalyzed crystallization induces $CaCO_3$ precipitation during the treatment process itself, so that future scaling potential can be greatly reduced. Finally,

reducing water heater temperature can be easily achieved by homeowners, and reduces scaling potentials by making all $CaCO_3$ solids more soluble at lower temperatures.

However, researchers are still dubious about the effects of magnetic antifouling, electronic antifouling and electrostatic devices on treating $CaCO_3$ scaling issues. These devices have been marketed for half a century, and vendors generally claim that these devices can reduce scaling by applying a magnetic field using either a permanent magnet or a temporary electromagnetic field generated by electron currents (Powell, 1998). A literature review by Powell (1998) suggests that there is little scientific data to support the claims of these devices, and a systematic experimental study by Limpert and Raber (1985) proved that eight electrostatic, magnetic and electromagnetic devices did not significantly reduce $CaCO_3$ scaling. However, Al Nasser et al. (2011) has observed a slight decrease in the scaling rates of $CaCO_3$ with the usage of electronic antifouling. They suggested that the conversion of calcite to vaterite, which is more soluble at 25 °C, might contribute to the decreased scaling rates of $CaCO_3$.

Table 1-8: Effects of common scaling prevention practices available for homes and buildings

Scaling prevention strategy	Advantages	Disadvantages	Mechanisms	References
Ion exchange softener	Frequently used; Softens water	Regeneration cycles add large amounts of salt to sewage and environment	Remove dissolved Ca	Edzwald, 2011
Nanofilters and Reverse osmosis membranes	High Ca^{2+} rejection (>90%); No net salinity addition to sewage	Energy intensive; Large amount of water is wasted	Remove dissolved Ca	Edzwald, 2011
Dutch pellet softening method	More effective than other alternative strategies	Water must initially be supersaturated with $CaCO_3$	Remove dissolved Ca	Schetters, 2013
Reduce water heater temperature	Lowers scaling potential in water heater; Greater savings on energy	Increases likelihood of pathogen formation (i.e. *Legionella pneumophila*)	Increase the solubility products of $CaCO_3$ solids	Plummer and Busenberg, 1982; ASHRAE, 2015
Magnetic antifouling devices	Inexpensive $CaCO_3$ control method; Little to no maintenance	No agreed upon mechanism of scaling inhibition; Questionable credibility	Weak scientific basis	Powell, 1998; Limpert and Raber. 1985; Al Nasser et al., 2011

1.6 Knowledge Gaps

This review re-evaluated $CaCO_3$ formation in potable water systems in the 21st century considering global warming, autogenous repair/leak clogging, use of corrosion inhibitors, and rising water temperatures in buildings and homes. Because of these emerging issues, research on $CaCO_3$ formation needs to be directed toward filling the following knowledge gaps: (1) Rising water heater temperatures and atmospheric CO_2 levels make it important to predict $CaCO_3$ formation in water systems. (2) Previous work needs to be updated to predict $CaCO_3$ scaling potential in presence of inhibitors and higher water heater set-point temperatures. (3) Scaling inhibitors such as phosphates or Zn^{2+} can control $CaCO_3$ formation, however scaling may be beneficial in protecting and repairing water pipelines.

1.7 References

Al-Deffeeri, N.S. (2007). Heat transfer measurement as a criterion for performance evaluation of scale inhibition in MSF plants in Kuwait. *Desalination*, 204, 423-436.

Al Nasser, W.N., Al Ruwaie, A.H., Hounslow, M.J., and Salman, A.D. (2011). Influence of electronic antifouling on agglomeration of calcium carbonate. *Powder Technology*, 206, 201-207.

Al Nasser, W.N., Shaikh, A., Morriss, C., Hounslow, M.J., and Salman, A.D. (2008). Determining kinetics of calcium carbonate precipitation by inline technique. *Chemical Engineering Science*, 63, 1381-1389.

American Society of Heating, Refrigerating, and Air-Conditioning Engineers (ASHRAE). (2015). *Legionellosis: Risk Management for Building Water Systems*. Atlanta, GA: ANSI/ASHRAE.

American Water Works Association (AWWA). (2012). *Buried No Longer: Confronting America's Water Infrastructure Challenge*. Denver, CO: AWWA.

American Water Works Association Research Foundation (AWWARF). (1996). *Internal Corrosion of Water Distribution Systems, 2nd ed*. Denver, CO: AWWA

Amor, M.B., Zgolli, D., Tlili, M.M., and Manzola, A.S. (2004). Influence of water hardness, substrate nature and temperature on heterogeneous calcium carbonate nucleation. *Desalination*, 166, 79-84.

Anderson, P.W. and Faust, S.D. (1972). Impact of drought on quality in a New Jersey water supply system. *Water Resources Bulletin (American Water Works Association)*, 8(4), 750-760.

Andritsos, N. and Karabelas, A.J. (2003). Calcium carbonate scaling in a plate heat exchanger in the presence of particles. *International Journal of Heat and Mass Transfer*, 46, 4613-4627.

Baylis, J.R. (1935). Treatment of water to prevent corrosion. *Journal American Water Works Association*, 29(2), 220-234.

Berner, R.A. and Morse, J.W. (1974). Dissolution kinetics of calcium carbonate in sea water IV. Theory of calcite dissolution. *American Journal of Science*, 274, 108-134.

Brazeau, R.H. and Edwards, M.E. (2011). A review of the sustainability of residential hot water infrastructure: public health, environmental impacts, and consumer drivers. *Journal of*

Green Building, 6(4), 77-95.

Bremere, I., Kennedy, M., Michel, P., Emmerik, R., Witkamp, G., and Schippers, J. (1999). Controlling scale in membrane filtration systems using a desupersaturation unit. *Desalination*, 124, 51-62.

Brezonik, P.L. and Arnold, W.A. (2011). *Water Chemistry: An Introduction to the Chemistry of Natural and Engineering Aquatic Systems*. New York, NY: Oxford University Press.

Buswell, A.M. (1916). A comparison of "temporary hardness" with alkalinity in natural waters. *Journal American Water Works Association*, 3(4), 959-961.

Cheong, W.C., Gaskell, P.H., and Neville, A. (2013). Substrate effect on surface adhesion/crystallisation of calcium carbonate. *Journal of Crystal Growth*, 363, 7-21.

Chou, L., Garrels, R.M., and Wollast, R. (1989). Comparative study of the kinetics and mechanisms of dissolution of carbonate minerals. *Chemical Geology*, 78, 269-282.

Clarkson, J.R., Price, T.J., and Adams, C.J. (1992). Role of metastable phases in the spontaneous precipitation of calcium carbonate. *Journal of the Chemical Society, Faraday Transactions*, 88(2), 243-249.

Clear, C.A. (1985). *The effects of autogenous healing upon the leakage of water through cracks in concrete*. Wexham, Slough, UK: Cement and Concrete Association.

Crabtree, M., Eslinger, D., Fletcher, P., Miller, M., Johnson, A., and King, G. (1999). Fighting scale – removal and prevention. *Oilfield Review*, autumn 1999, 30-45.

Dąbrowski, W., Buchta, R., Dąbrowska, B., and Mackie, R.I. (2010). Calcium carbonate equilibria in water supply systems. *Environment Protection Engineering*, 36(2), 75-94.

Dalas, E., Kallitsis, J., and Koutsoukos, P.G. (1988). The crystallization of calcium carbonate on polymeric substrates. *Journal of Crystal Growth*, 89, 287-294.

Dalas, E. and Koutsoukos, P.G. (1990). Calcium carbonate scale formation and prevention in a flow-through system at various temperatures. *Desalination*, 78, 403-416.

Davis, K.J., Dove, P.M., and De Yoreo, J.J. (2000). The role of Mg^{2+} as an impurity in calcite growth. *Science*, 290, 1134-1137.

DeMartini, F.E. (1938). Corrosion and the Langelier calcium carbonate saturation index. *Journal American Water Works Association*, 30(1), 85-111.

Dobersek, D. and Goricanec, D. (2007). Influence of water scale on thermal flow losses of domestic applicances. *International Journal of Mathematical Models and Methods in*

Applied Sciences, 2(1), 55-61.

Edvardsen, C. (1999). Water permeability and autogenous healing of cracks in concrete. *ACI Materials Journal*, 96(4), 448-454.

Edzwald, J.K. (2011). *Water Quality and Treatment: A Handbook on Drinking Water*. Denver, CO: AWWA.

Energy Star (United States Department of Energy and United States Environmental Protection Agency). (n.d.). 2014 Federal tax credits. http://www.energystar.gov/about/federal_tax_credits/2014_federal_tax_credits (Accessed 12 Nov. 2015).

Evans, C.D., Chapman, P.J., Clark, J.M., Monteith, D.T., and Cresser, M.S. (2006). Alternative explanations for rising dissolved organic carbon export from organic soils. *Global Change Biology*, 12, 2044-2053.

Federal Highway Administration Research and Technology (FHWA). (2002). *Corrosion Costs and Preventive Strategies in the United States*. Washington, D.C.: U.S. Department of Transportation.

Förster, M., Augustin, W., and Bohnet, M. (1999). Influence of the adhesion force crystal/heat exchanger surface on fouling mitigation. *Chemical Engineering and Processing*, 38, 449-461.

Fox, P. and Abbaszadegan, M. (2013). *Impact of Scale Formation on Biofilm Growth in Premise Plumbing*. Naples, FL: Salt Institute.

Freeman, C., Evans, C.D., and Monteith, D.T. (2001). Export of organic carbon from peat soils. *Nature*, 412, 785.

Freeman, C., Fenner, N., Ostle, N.J., Kang, H., Dowrick, D.J., Reynolds, B., Lock, M.A., Sleep, D., Hughes, S., and Hudson, J. (2004). Export of dissolved organic carbon from peatlands under elevated carbon dioxide levels. *Nature*, 430, 195-198.

Garrett-Price, B.A., Smith, S.A., Watts, R.L., and Knudsen, J.G. (1985). *Fouling of Heat Exchangers: Characteristics, Costs, Prevention, Control, and Removal*. Park Ridge, NJ: Noyes Publications.

Gebauer, D., Kellermeier, M., Gale, J.D., Bergström, L., and Cölfen, H. (2014). Pre-nucleation clusters as solute precursors in crystallisation. *Chemical Society Reviews*, 43(7), 2348-2371.

Gebauer, D., Völkel, A., and Cölfen, H. (2008). Stable prenucleation calcium carbonate clusters. *Science*, 322(5909), 1819-1822.

Ghizellaoui, S. and Euvrard, M. (2008). Assessing the effect of zinc on the crystallization of calcium carbonate. *Desalination*, 220, 394-402.

Githens, R.E., Minor, W.R., and Tomsic, V.J. (1965). Flexible-tube heat exchangers. *Chemical Engineering Progress*, 61(7), 55.

Goudey, R.F. (1933). The chemistry of water softening. *Journal American Water Works Association*, 25(9), 1203-1206.

Greth, J.C.W. (1910). *Water Purification Facts for Steam Users*. Pittsburgh, PA: Wm. B. Schaife & Sons Co.

Gwon, E., Yu, M., Oh, H., and Ylee, Y. (2003). Fouling characteristics of NF and RO operated for removal of dissolved matter from groundwater. *Water Research*, 37, 2989-2997.

Hasson, D. and Karmon, M. (1981). *Method for calcite coating on the inner surface of pipes*. United States Patent no. US4264651

Hatch, G.B. (1942). *Control of calcium carbonate deposition for corrosion inhibition*. United States Patent no. US2299748.

Hearn, N. (1998). Self-sealing, autogenous healing and continued hydration: what is the difference? *Materials and Structures*, 31, 563-567.

Hehner, O. (1883). Estimation of hardness without soap solution. *Analyst*, 8, 77-81.

Hoch, A.R., Reddy, M.M., and Aiken, G.R. (2000). Calcite crystal growth inhibition by humic substances with emphasis on hydrophobic acids from the Florida Everglades. *Geochimica et Cosmochimica Acta*, 64, 61-72.

Holm, T.R. and Edwards, M. (2003). Metaphosphate reversion in laboratory and pipe-rig experiments. *Journal American Water Works Association*, 95(4), 172-178.

Houska, C. (2007). Deicing salt – recognizing the corrosion threat. *International Molybdenum Association, Pittsburgh, TMR Consulting*.

Jaćimović, N., Stamenić, M., Kolendić, P., Đorđević, D., Radanov, B., and Vladić, L. (2015). A novel method for the inclusion of pipe roughness in the Hazen-Williams Equation. *FME Transactions*, 43, 35-39.

Kazmierczak, T.F., Tomson, M.B., and Nancollas, G.H. (1982). Crystal growth of calcium carbonate. A controlled composition kinetic study. *The Journal of Physical Chemistry*,

86, 103-107.

Kellermeier, M., Glaab, F., Klein, R., Melero-García, E., Kunz, W., and García-Ruiz, J.M. (2013). The effect of silica on polymeric precipitation of calcium carbonate: an on-line energy-dispersive x-ray diffraction (EDXRD) study. *Nanoscale*, 5, 7054-7065.

Keysar, S., Semiat, R., Hasson, D., and Yahalom, J. (1994). Effect of surface roughness on the morphology of calcite crystallization in mild steel. *Journal of Colloid and Interface Science*, 162, 311-319.

Kralj, D. and Vdović, N. (2000). The influence of some naturally occurring minerals on the precipitation of calcium carbonate polymorphs. *Water Research*, 34(1), 179-184.

Krappe, J.M. (1940). *Scale Formation in Water Heaters*. Lafayette, IN, USA: Purdue University.

Kutty, P.C.M., Nomani, A.A., and Al-Sulami, S. (1992). Simple experimental method to determine $CaCO_3$ precipitation tendency in desalinated water. In *First Gulf Water Conference*, October, 685-708, Dubai, UAE.

Lam, R.S.K., Charnock, J.M., Lennie, A., and Meldrum, F.C. (2007). Synthesis-dependent structural variations in amorphous calcium carbonate. *CrystEngComm*, 9, 1226-1236.

Langelier, W.F. (1936). The analytical control of anti-corrosion water treatment. *Journal American Water Works Association*, 28(10), 1500-1521.

Larson, T.E. and Skold, R.V. (1957). Corrosion and tuberculation of cast iron. *Journal American Water Works Association*, 49(10), 1294-1302.

Larson, T.E. and Skold, R.V. (1958). Laboratory studies relating mineral quality of water to corrosion of steel and cast iron. *Corrosion*, 14(6), 43-46.

Lebron, I. and Suarez, D.L. (1996). Calcite nucleation and precipitation kinetics as affected by dissolved organic matter at 25 °C and pH > 7.5. *Geochimica et Cosmochimica Acta*, 60(15), 2765-2776.

Limpert, G.J.C. and Raber, J.L. (1985). Tests of nonchemical scale control devices in a once-through system. *Materials Performance*, 24(10), 40-45.

Lin, Y. and Singer, P.C. (2005a). Inhibition of calcite crystal growth by polyphosphates. *Water Research*, 39, 4835-4843.

Lin, Y. and Singer, P.C. (2005b). Effect of seed material and solution composition on calcite precipitation. *Geochimica et Cosmochimica Acta*, 69(18), 4495-4504.

Lin, Y. and Singer, P.C. (2006). Inhibition of calcite precipitation by orthophosphate: speciation

and thermodynamic considerations. *Geochimicha et Cosmochimica Acta*, 70, 2530-2539.

Lin, Y. and Singer, P.C. (2009). Effect of Mg^{2+} on the kinetics of calcite crystal growth. *Journal of Crystal Growth*, 312, 136-140.

Lin, Y., Singer, P.C., and Aiken, G.R. (2005). Inhibition of calcite precipitation by natural organic material: kinetics, mechanism, and thermodynamics. *Environmental Science and Technology*, 39, 6420-6428.

Lioliou, M.G., Paraskeva, C.A., Koutsoukos, P.G., and Payatakes, A.C. (2007). Heterogeneous nucleation and growth of calcium carbonate on calcite and quartz. *Journal of Colloid and Interface Science*, 308, 421-428.

Liu, C.Z., Lin, C.H., Yeh, M.S., Chao, Y.M., and Shen, P. (2010). Surface modification and planar defects of calcium carbonates by magnetic water treatment. *Nanoscale Research Letters*, 5, 1982-1991.

Logsdon, G.S., Hess, A.F., Chipps, M.J., and Rachwal, A.J. (2002). *Filter Maintenance and Operations Guidance Manual*. Denver, CO: AWWA.

MacAdam, J. and Parsons, S.A. (2004a). Calcium carbonate scale formation and control. *Reviews in Environmental Science and Bio/Technology*, 3, 159-169.

MacAdam, J. and Parsons, S.A. (2004b). Calcium carbonate scale control, effect of material and inhibitors. *Water Science and Technology*, 49(2), 153-159.

Matty, J.M. and Tomson, M.B. (1988). Effects of multiple precipitation inhibitors on calcium carbonate nucleation. *Applied Geochemistry*, 3(5), 549-556.

McCauley, R.F. (1960). Calcite coating protects water pipes. *Water & Sewage Works*, 107(7), 276-281.

Morse, J.W. (1983). The kinetics of calcium carbonate dissolution and precipitation. *Reviews in Mineralogy and Geochemistry*, 11, 227-264.

Morse, J.W. and Arvidson, R.S. (2002). The dissolution kinetics of major sedimentary carbonate minerals. *Earth Science Reviews*, 58(1-2), 51-84.

Morse, J.W., Arvidson, R.S., and Lüttge, A. (2007). Calcium carbonate formation and dissolution. *Chemical Reviews*, 107(2), 342-381.

Mosley, L.M. (2015). Drought impacts on the water quality of freshwater systems; review and integration. *Earth-Science Reviews*, 140, 203-214.

Müller-Steinhagen, H. (2000). *Heat Exchanger Fouling: Mitigation and Cleaning Technologies*.

Rugby, Warwickshire, UK: Institution of Chemical Engineers.

Müller-Steinhagen, H. and Zhao, Q. (1997). Investigation of low fouling surface alloys made by ion implantation technology. *Chemical Engineering Science*, 52(19), 3321-3332.

Mullin, J.W. (2001). Nucleation. In: *Crystallization, 4th Ed.* Oxford, UK: Butterworth-Heinemann.

Nancollas, G.H. and Reddy, M.M. (1971). The crystallization of calcium carbonate – II. Calcite growth mechanism. *Journal of Colloid and Interface Science*, 37(4), 824-830.

National Research Council (NRC). (1982). *Drinking Water and Health, Vol. 4*. Washington, DC: National Academy Press.

Neville, A., Hodgkiess, T., and Morizot, A.P. (1999). Electrochemical assessment of calcium carbonate deposition using a rotating disk electrode (RDE). *Journal of Applied Electrochemistry*, 29, 455-462.

Ng, J.D., Lorber, B., Witz, J., Théobald-Dietrich, A., Kern, D., and Giegé, R. (1996). The crystallization of biological macromolecules from precipitates: evidence for Ostwald ripening. *Journal of Crystal Growth*, 168, 50-62.

Nielson, L.C., De Yoreo, J.J., and DePaolo, D.J. (2013). General model for calcite growth kinetics in the presence of impurity ions. *Geochimica et Cosmochimica Acta*, 115, 100-114.

Norton, J.F. and Knowles, H.I. (1916). A study of indicators for the determination of temporary hardness in water. *Journal of the American Chemical Society*, 38(4), 877-884.

Ogino, T., Suzuki, T., and Sawada, K. (1987). The formation and transformation mechanism of calcium carbonate in water. *Geochimica et Cosmochimica Acta*, 51(10), 2757-2767.

Pääkkönen, T.M., Riihimäki, M., Puhakka, E., Muurinen, E., Simonson, C.J., and Keiski, R.L. (2009). Crystallization fouling of $CaCO_3$ – effect of bulk precipitation on mass deposition on the heat transfer surface. *Proceedings of International Conference on Heat Exchanger Fouling and Cleaning VIII*, 209-216.

Parks, J., Edwawrds, M, Vikesland, P., and Dudi, A. (2010). Effects of bulk water chemistry on autogenous healing of concrete. *Journal of Materials in Civil Engineering*, 22(5), 515-524.

Pitman, R.M. (2006). Wood ash use in forestry – a review of the environmental impacts. *Forestry*, 79(5), 563-588.

Plummer, L.N. and Busenberg, E. (1982). The solubilities of calcite, aragonite and vaterite in CO_2-H_2O solutions between 0 and 90 °C, and an evaluation of the aqueous model for the system $CaCO_3$-CO_2-H_2O. *Geochimica et Cosmochimica Acta*, 46, 1011-1040.

Plummer, L.N., Wigley, T.M.L., and Parkhurst, D.L. (1978). The kinetics of calcite dissolution in CO_2-water systems at 5° to 60°C and 0.0 to 1.0 atm CO_2. *American Journal of Science*, 278, 179-216.

Pollio, M.V. (1960). *Vitruvius: The Ten Books on Architecture*. Translated by Morgan, M.H. Cambridge, MA: Harvard University Press.

Powell, M.R. (1998). Magnetic water and fuel treatment: myth, magic, or mainstream science? *Skeptical Inquirer*, 22.1.

Primus, N.S. and Hunhoff, R. (1972). *Method for Lining Pipes with Calcite*. United States Patent no. US3640759

Puckorius, P.R. and Brooke, J.M. (1991). A new practical index for calcium carbonate scale prediction in cooling tower systems. *Corrosion*, 47(4), 280-284.

Reddy, M.M., Plummer, L.N., and Busenberg, E. (1981). Crystal growth of calcite from calcium bicarbonate solutions at constant P_{CO2} and 25 °C: a test of a calcite dissolution model. *Geochimica et Cosmochimica Acta*, 45, 1281-1289.

Reddy, M.M. and Wang, K.K. (1980). Crystallization of calcium carbonate in the presence of metal ions: I. Inhibition by magnesium ion at pH 8.8 and 25 °C. *Journal of Crystal Growth*, 50(2), 470-480.

Rodriguez-Hornedo, N. and Murphy, D. (1999). Significance of controlling crystallization mechanisms and kinetics in pharmaceutical systems. *Pharmaceutical Sciences*, 88(7), 651-660.

Roqué, J., Molera, J., Vendrell-Saz, M., and Salvadó, N. (2004). Crystal size distributions of induced calcium carbonate crystals in polyaspartic acid and *Mytilus edulis* acidic organic proteins aqueous solutions. *Journal of Crystal Growth*, 262, 543-553.

Rossum, J.R. and Merrill, D.T. (1983). An evaluation of the calcium carbonate saturation indexes. *Journal American Water Works Association*, 75(2), 95-100.

Roy, S. and Edwards, M.E. (2015). Role of water hardness precipitation and flashing cavitation in erosion corrosion of copper in potable water systems. In *134th AWWA Annual Conference and Exposition (ACE)*, 7-8 June, Anaheim, CA.

Royer, M., Davidson, J.H., Francis, L.F., and Mantell, S.C. (2010). Shear induced removal of calcium carbonate scale from polypropylene and copper tubes. *Journal of Solar Energy Engineering*, 132, 011013 (9 pages).

Ryznar, J.W. and Langelier, W.F. (1944). A new index for determining amount of calcium carbonate scale formed by a water [with discussion]. *Journal American Water Works Association*, 36(4), 472-486.

Sawada, K. (1997). The mechanisms of crystallization and transformation of calcium carbonates. *Pure and Applied Chemistry*, 69(5), 921-928.

Schetters, M.J.A. (2013). *Grinded Dutch calcite as seeding material in the pellet softening process* (Master's thesis). Delft University of Technology, Delft, Netherlands.

Schneider, C.R. and Stumm, W. (1964). Evaluation of corrosion in distribution systems. *Journal American Water Works Association*, 56(5), 621-632.

Schock, M.R. (1989). Understanding corrosion control strategies for lead. *Journal American Water Works Association*, 81(7), 88-100.

Seneviratne, M. (2007). *A Practical Approach to Water Conservation for Commercial and Industrial Facilities*. Elsevier.

Shakkthivel, P. and Vasudevan, T. (2006). Acrylic acid-diphenylamine sulfonic acid copolymer threshold inhibitor for sulfate and carbonate scales in cooling water systems. *Desalination*, 197, 179-189.

Shanaghan, P.E. (2012). Assessing drinking water infrastructure need. *Journal American Water Works Association*, 104(8), 14-15.

Sherman, L.A. and Barak, P. (1999). Solubility and dissolution kinetics of dolomite in Ca-Mg-HCO_3/CO_3 solutions at 25 °C and 0.1 MPa carbon dioxide. *Soil Science Society of America Journal*, 64(6), 1959-1968.

Stumm, W. (1956). Calcium carbonate deposition at iron surfaces. *Journal American Water Works Association*, 48(3), 300-310.

Tang, M., Triantafyllidou, S., and Edwards, M. (2013). In situ remediation of leaks in potable water supply systems. *Corrosion Review*, 31(3-6), 105-122.

Tang, M., Triantafyllidou, S., and Edwards, M. (2015). Autogenous metallic pipe leak repair in potable water systems. *Environmental Science and Technology*, 49(14), 8697-8703.

Thomas, M., Hayden, A.C.S, and MacKenzie, D. (2006). Reducing GHG emissions through

efficient water heating technologies. In *EIC Climate Change Technology, 2006 IEEE*, 10-12 May, Ottawa, ON.

Troup, D.H. and Richardson, J.A. (1978). The link between corrosion and calcium carbonate scaling susceptibilities of heat transfer surfaces. *Werkstoffe und Korrosion*, 29, 312-320.

United States Department of Energy (U.S. DoE). (n.d.). Tankless or demand-type water heaters. http://energy.gov/energysaver/tankless-or-demand-type-water-heaters (Accessed 10 Nov. 2015).

United States Environmental Protection Agency (U.S. EPA). (1992). *Lead and Copper Rule Guidance Manual Volume II: Corrosion Control Treatment*. Washington, DC: Office of Water.

United States Environmental Protection Agency (U.S. EPA). (2000). *Information Collection Rule (ICR) Auxiliary 1 Database, Version 5.0 Query Tool, Version 2.0.* Washington, DC: NTIS.

Wada, N., Yamashita, K., and Umegaki, T. (1995). Effects of divalent cations upon nucleation, growth and transformation of calcium carbonate polymorphs under conditions of double diffusion. *Journal of Crystal Growth*, 148, 297-304.

Wang, Y., Davidson, J., and Francis, L. (2005). Scaling in polymer tubes and interpretation for use in solar water heating systems. *Journal of Solar Energy Engineering*, 127, 3-14.

Water Quality Research Foundation (WQRF). (2011). *Softened Water Benefits Study (Energy and Detergent Savings)*. Lisle, IL: Water Quality Association.

Wiggin, T.H., Norcom, G.D., Glace, I.M., Davis, D.E., Olson, H.M., Ackerman, J.W., and Alexander, C. (1938). Corrosion control – studies and operating experiences: a round table discussion. *Journal American Water Works Association*, 30(8), 1342-1387.

Wojtowicz, J.A. (2001). A revised and updated saturation index equation. *Journal of the Swimming Pool and Spa Industry*, 3(1), 28-34.

Wolf, S.E., Leiterer, J., Kappl, M., Emmerling, F., and Tremel, W. (2008). Early homogeneous amorphous precursor stages of calcium carbonate and subsequent crystal growth in levitated droplets. *Journal of the American Chemical Society*, 130(37), 12342-12347.

Wray, J.L. and Daniels, F. (1957). Precipitation of calcite and aragonite. *Journal of the American Chemical Society*, 79(9), 2031-2034.

Wu, Z., Davidson, J.H., and Francis, L.F. (2010). Effect of water chemistry on calcium carbonate

deposition on metal and polymer surfaces. *Journal of Colloid and Interface Science*, 343, 176-187.

Wu, Z., Francis, L.F., and Davidson, J.H. (2009). Scale formation on polypropylene and copper tubes in mildly supersaturated tap water. *Solar Energy*, 83, 636-645.

Xyla, A.G., Giannimaras, E.K., and Koutsoukos, P.G. (1991). The precipitation of calcium carbonate in aqueous solutions. *Colloids and Surfaces*, 53, 241-255.

Yang, Q., Ding, J., and Shen, Z. (2000). Investigation of calcium carbonate scaling on ELP surface. *Journal of Chemical Engineering of Japan*, 33(4), 591-596.

Yang, Q., Liu, Y., Gu, A., Ding, J., and Shen, Z. (2001). Investigation of calcium carbonate scaling inhibition and scale morphology by AFM. *Journal of Colloid and Interface Science*, 240, 608-621.

Yang, Q., Liu, Y., Gu, A., Ding, J., and Shen, Z. (2002). Investigation of induction period and morphology of $CaCO_3$ fouling on heated surface. *Chemical Engineering Science*, 57, 921-931.

Chapter 2: Autogenous Leak Repair via Inert Particle Clogging

2.1 Introduction

Fixing the aging water infrastructure in the United States (U.S.) is one of the grand challenges of the 21st century. As many systems approach 100 years old, they have begun to fail at an alarming rate. Nearly 5.9 billion gallons of water are lost every day in our water infrastructure due to leaks, main breaks, and inaccurate meters (CNT, 2013). Consequences of small leaks, if they grow larger, can include increased water loss and eventually catastrophic and expensive water main breaks—240,000 main breaks occur in the U.S. every year (ASCE) (2013). Dirt and pathogens can also be drawn into water mains through leaks (AWWARF, 2001), during brief depressurization events (Walski and Lutes, 1994). Finally, water main leaks and breaks can cause property damage to nearby buildings and infrastructure (i.e. flooding, pothole formation), and undermine roads.

In 2013, the ASCE gave the U.S. drinking water infrastructure a grade of D (ASCE, 2013). It is estimated that the cost of repairing our existing infrastructure is $200 billion over the next 20 years (Shanaghan, 2012). Conventional methods include repair, rehabilitation, and replacement, which are effective but time consuming and expensive. Therefore, there is a continued demand for a more cost-effective solution to fixing our leaking water infrastructure, as well as a desire to reduce the frequency of leaks in the first place.

Novel methods of *in situ* repair of leaks have been proposed as promising temporary measure (Tang et al., 2013) and have shown effective in lab-scale studies in concrete (Edvardsen, 1999; Parks et al., 2010) and metallic (Tang et al., 2015) pipes. There are three mechanisms: (1) Metallic corrosion, where leaks are repaired through the formation of iron or copper corrosion precipitates, (2) precipitation, where leaks are repaired by clogging with water-formed particles such as $CaCO_3$ or hydration products from concrete, and (3) physical clogging, where leaks are repaired via blockage by waterborne particles. Among these three mechanisms, physical clogging is of the potentially greatest application, because it might be applied to a wide range of pipe materials including inert materials such as aged concrete and PVC (Tang et al., 2013).

We conceptualize blockage of small pipe leaks by waterborne particles as a two step process including 1) particle transport to the leak, and 2) deposition and formation of blockages within leaks (Figure 2-1). The first step is practically important because, in concept, the leaks might be quite distant from the point of introduction to the system, and the particles will be prevented from reaching the leak if it settles out of the bulk fluid or adheres to the pipe wall too early. Even when a particle settles out of the bulk fluid, it is not necessarily stationary as there are still mechanisms by which it can be transported through a pipe. These mechanisms include rolling/sliding (Soepyan et al., 2013) and saltation, where a settled particle is resuspended before resettling (Cabrejos and Klinzing, 1994). To the extent particles do settle, the leaks at the top of the pipe will be more difficult to clog. The ***critical deposit velocity*** describes the minimum velocity required to keep a particle suspended in flow (Thomas, 1979) and it primarily depends on particle size, particle density, and pipe diameter (Turian et al., 1987). Water velocity through a distribution system might not be able to vary significantly from its design flow, thus in practical application of attempted leak repair via particle clogging, the particle type and size would be the controlled variables.

After the particle arrives at the leak, it must be capable of clogging it (Figure 2-1). There are several mechanisms by which this can occur. (1) If the particle is larger than the leak, it can become trapped in the leak and held by pressure via a sieving type mechanism. Similarly, smaller, destabilized particles can flocculate into a larger particle capable of clogging. (2) If particles are smaller than the leak, they can build up around it and gradually reduce the leak size (Hajra et al., 2002). (3) Using analogies to filtration, the speed of build-up in or around the leaks is expected to be maximum if the particles are nearly zero surface charge.

Different water chemistry and flow parameters can affect a particle's capability of clogging leaks, especially when the particles are smaller than the leak. Agbangla et al. (2012) found that the type of pore clogging (i.e. arching, dendrite formation, or dense deposit formation) is dependent on flow patterns, particle concentration, and physical interactions between the particle and pore. A model constructed by Wyss et al. (2006) suggests that the pore clogging rate is controlled by a critical number of particles that pass through a pore. The critical number is strongly influenced by particle diameter (Wyss et al., 2006). This is consistent with other studies that found solutions with a lower concentration of larger particles clogs pores more rapidly than solutions with greater

concentration of smaller particles (Hajra et al., 2002; Mustin and Stoeber, 2010). Finally, the water's ionic strength affects a particle's ability to clog pores. Waters with high ionic strength will compress the double layer surrounding particles, increasing their likelihood of adhesion upon contact with one another and the leak wall (Hajra et al., 2002; Dersoir et al., 2015). Other methods of particle agglomeration, such as neutralizing the zeta potential, may also prove to be conducive to clogging (Tang et al., 2013). However, in a potable water system, the larger particles formed by agglomeration may settle out of a solution or adhere to the pipe wall before they reach a leak, which in turn eliminates the likelihood of clogging a leak. Therefore, the particle size, surface charge, and solution ionic strength may need to be optimized to maximize clogging rate at a given distance downstream from a point at which particles are added to the water.

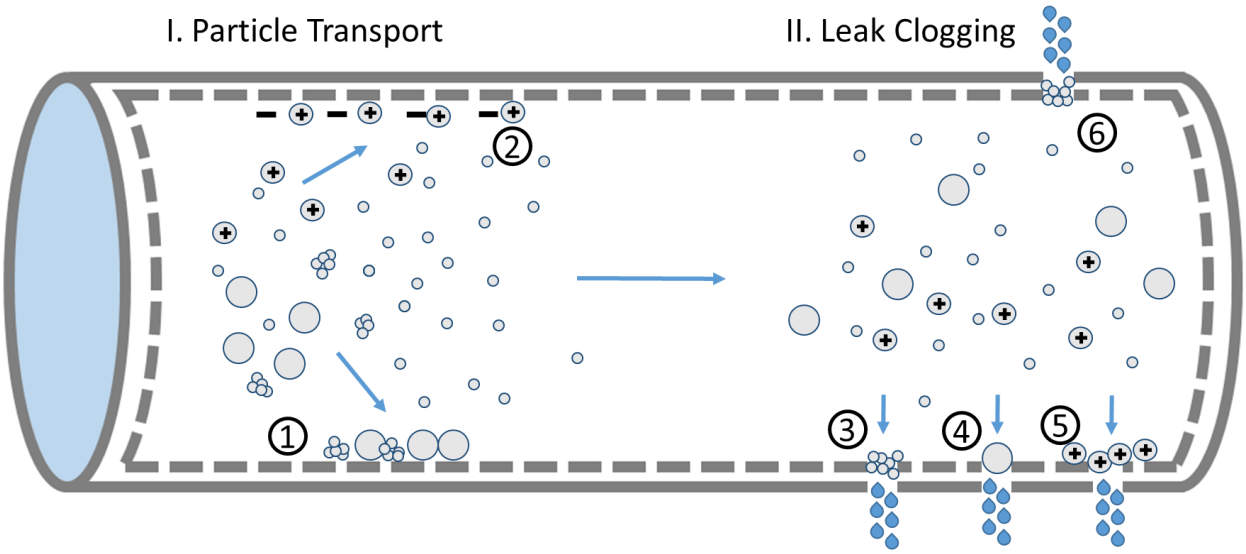

Figure 2-1 Overview of factors important to particle transport and leak clogging in pipes: (1) Large particles and flocculated smaller particles may settle before reaching the leak. (2) Charged particles can stick to the walls of the pipe if conditions are suitable in terms of charge and transport. (3) Particles smaller than the leak can clog it by sticking to the wall of the leak and gradually building up inside it. (4) A single large particle or a floc of smaller particles can clog the leak provided it has a greater diameter. (5) Particles of a similar charge can coat a leak as a monolayer without particle build-up. (6) Certain flow conditions (i.e. turbulence) can allow particles suspended throughout the pipe depth to clog leaks regardless of leak orientation.

The overall goal of this work is to assess leak repair via the particle clogging mechanism. Both the particle transport and particle clogging steps of this mechanism are tested simultaneously. Specifically, this study aims to simulate pinhole (circular, 250 μm diameter) leaks in a bench scale water-recirculating system using two model inert particles including silica and alumina.

2.2 Materials and Methods

Particle Analysis

Silica particles were ground Sil-Co-Sil 75 and fine ground Min-U-Sil 40, donated by U.S. Silica. Aluminum oxide (alumina) particles was purchased from Sigma Aldrich (CAS number 1344-28-1), sized -325 mesh with purity ≥ 99%. The crystal polymorph of the silica and alumina were analyzed by X-ray diffraction (Panalytical X'Pert 3 Powder). Particle size distributions were measured using a HORIBA LA-300 Laser Diffraction Particle Size Distribution Analyzer. A 10.12 ± 0.06 μm diameter polystyrene particle was used as a size standard to confirm particle sizing accuracy. Particle zeta potential was determined by measurement of electrophoretic mobility using a Zeta-Meter 3.0+ instrument. Accurate zeta potential measurement was confirmed using a 100 mg/L Min-U-Sil 40 standard in a 100 mg/L NaCl solution per manufacturer instruction.

Solution Compositions

A total of nine different solutions were prepared in nanopure water for the leak repair experiments including one control (Table 2-1) with the highest concentration of each constituent used in the high ionic strength waters. Low ionic strength solutions represented potable water quality in a real water distribution system. The pH of the low ionic strength solutions ranged from 5.5 to 10.3 without any particles. NaCl was added to the 0.1 mM $NaHCO_3$ and 1 mM $NaHCO_3$ waters to ensure each of low ionic strength solutions had a nearly uniform ionic strength. The pH of each water measured by an Oakton 110 Series pH meter. Ionic strength for each solution was calculated using Mineql+.

Table 2-1 Composition of waters used in leak clogging experiments

Name	Composition	Ionic strength (M)[1]
Control		
Control	94 mM K_2HPO_4 + 38.5 mM KH_2PO_4 + 25 mM $NaHCO_3$ + 10.7 mM KOH	0.335
High ionic strength		
pH 7 Buffer	61.5 mM K_2HPO_4 + 38.5 mM KH_2PO_4	0.199
pH 8 Buffer	94 mM K_2HPO_4 + 6 mM KH_2PO_4	0.240
pH 9.6 Buffer	25 mM $NaHCO_3$ + 5 mM KOH	0.035
pH 10 Buffer	25 mM $NaHCO_3$ + 10.7 mM KOH	0.045
Low ionic strength		
3 mM NaCl	3 mM NaCl	$3.00x10^{-3}$
0.1 mM $NaHCO_3$	0.1 mM $NaHCO_3$ + 2.9 mM NaCl	$3.00x10^{-3}$
1 mM $NaHCO_3$	1 mM $NaHCO_3$ + 2 mM NaCl	$3.07x10^{-3}$
1 mM Na_2CO_3	1 mM Na_2CO_3	$2.61x10^{-3}$

[1]Ionic strength calculated using Mineql+ in a closed system

Leak Repair Experimental Design

A series of 17 separate leak repair experiments and 1 control experiment were conducted to study the repair of leaks by particle clogging: 4 experiments were conducted using Sil-Co-Sil 75 in the high ionic strength waters, 8 were conducted using Min-U-Sil 40 in the high ionic strength and low ionic strength waters, 4 were conducted using alumina particles in the low ionic strength waters, and 1 was conducted using alumina particles that remained unsettled 60 minutes after mixing a 5 g/L alumina stock solution. No particles were added to the control experiment.

Each experiment was conducted in a water-recirculation system (Figure 2-2) in which water was pumped (MasterFlex L/S series peristaltic pump) through a system made from rigid PVC tubing (3/8" o.d. x 1/4" i.d.). Total system pressure was adjusted to 20 psi via a needle valve and was

monitored using a pressure gauge. Three 1 m long segments of flexible tubing were installed to maintain constant pressure. After the valve, the water was redirected back into the stirred vessel.

Leaks were simulated using borosilicate, heavy wall capillaries (3 mm o.d. x 0.25 mm i.d.) purchased from Vitrocom. 3 mm diameter holes were drilled into a 6 in. long portion of PVC tubing. The capillaries were cut to lengths of 2 cm and adhered to the holes using epoxy glue. Leaks were oriented on the top, side, and bottom walls of the tubing to test leak clogging at different orientations. Each orientation was tested in triplicate, making a total of nine leaks in each experiment. Flexible, 3 mm i.d. tubing was placed at the end of each capillary to redirect the leaked water back into the stirred vessel.

Before starting each experiment, silica or alumina particles were added into the synthesized solutions (Table 2-1) in the reservoir. For experiments using silica particles, an initial turbidity of approximately 6-7 NTU was achieved by adding 4-5 mL of the silica stock solution (5 g/L) into 750 mL of the solution. For the experiments using alumina particles, an initial alumina concentration of 250 mg/L was achieved by adding alumina stock solution (5 g/L) into 855 mL of the synthesized solution. An additional experiment was conducted on smaller alumina particles that have a lower tendency to settle. For this experiment, the alumina stock solution was stirred vigorously before settling for 60 minutes. Then, 45 mL were drawn from the surface of the stock solution, which contained the unsettled alumina particles, and transferred to 855 mL of the synthesized solution via pipette.

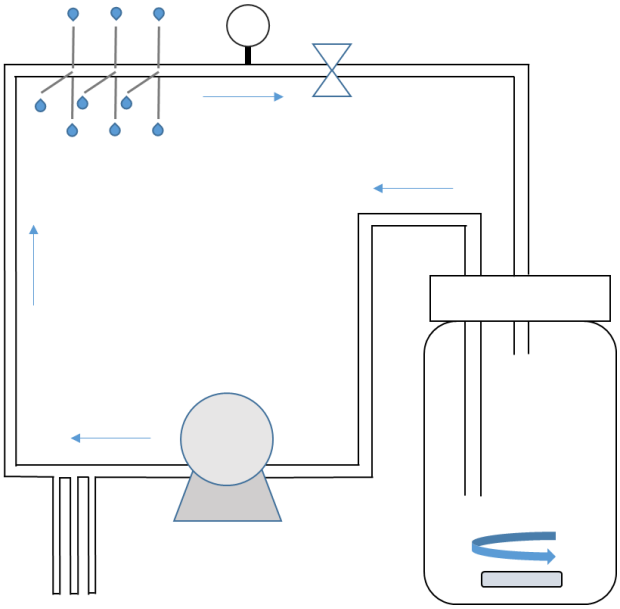

Figure 2-2 Recirculation system setup: Synthesized solutions were well mixed with silica or alumina particles in a reservoir, before being pumped through the recirculation system using a peristaltic pump. A pressure tank was placed after the pump to maintain 20 psi and reduce fluctuations in pressure. Capillaries (250 um i.d.) simulated pipe leaks, and the leaked water was rerouted back to the stirred container via flexible tubing (not shown). A pressure gauge and needle valve were used to monitor and regulate system pressure.

Leak Monitoring

The leak rate through each capillary was measured daily for 10 days. The water in each vessel was also replaced daily with freshly made synthesized water and dosed to the same particle concentration, with the exception of the unsettled particle experiment, which was only replaced once at day 6. Two turbidity measurements were taken daily, right before and after each water replacement. Turbidity was measured on a Hach 2100N Turbidimeter which was regularly calibrated using a hydrazine sulfate turbidity standard. Microscope photos of the leaks, simulated by glass capillaries, were taken using an MU300 3 megapixel camera mounted on an AmScope IN300TC optical microscope.

2.3 Results and Discussion

Particle Characterization

Particle size distributions were measured for Min-U-Sil 40, Sil-Co-Sil 75, and alumina in each of the solutions used in the clogging experiments (Table 2-2). As expected given that the pH of the experiments was much higher than the pH_{PZC} (Schwarz et al., 1984), the size of the Min-U-Sil 40 and Sil-Co-Sil 75 particles were not significantly affected by the solution chemistry. In contrast, the alumina particles had higher mean diameter than the silica particles, and had a range of zeta potentials from moderately negative (-22.2 mV), near neutral (-7.1 and 12.0 mV), and highly positive (36.0 mV) consistent with pH_{pzc} = 7.1 correspondingly varied in size due to coagulation (Schwarz et al., 1984). Thus, the silica particles essentially allowed for study of fixed particle size and settling velocity on clogging rates in different solutions, whereas the alumina allowed these parameters to be varied, thereby representing extremes of behavior for particles that could be used in practice. In one experiment, the fraction of alumina unsettled after 60 minutes of stagnation was collected, creating a suspension with much lower particle size and initial settling velocity than the other alumina solutions.

As discussed in the introduction, it was hypothesized that larger particles would be more efficient at clogging pores than small particles at the same volume fraction (Hajra et al., 2002; Mustin and Stoeber, 2006; Wyss et al., 2010). On the other hand, if the particles are too large, they have a higher tendency to settle out of the water flowing through the pipe before they arrive at a leak. The ***critical settling velocity***, or the minimum fluid velocity required to keep particles from settling in a pipeline, was modeled using the approach of Danielson (2007) (Figure 2-3). Larger diameter pipes require higher flow velocities to keep particles suspended. For the particles tested herein, the model predicts that all the alumina and silica particles in a real pipe system with a large diameter such as the Delaware Aqueduct will settle, including particles as small as 10 nm (Figure 2-3A, 2-3C). But for the very small diameter tube systems tested herein, the average-sized particles in each of these experiments are predicted to remain in suspension, with the alumina particles being closer to the critical settling velocity than silica (Figure 2-3B, 2-3D).

Table 2-2: Mean particle size and zeta potential measurements on particles used in each solution

Solution	Mean diameter (μm)	Mean standard deviation (μm)	Zeta potential (mV)
Min-U-Sil 40			
Nanopure	17.4	9.6	N/A
pH 7 Buffer	15.3	12.5	-31.6
pH 8 Buffer	13.7	12.3	-30.5
pH 9.6 Buffer	14.1	12.4	-40.0
pH 10 Buffer	16.2	13.3	-36.0
3 mM NaCl	17.3	9.5	-34.1
0.1 mM $NaHCO_3$	15.5	8.6	-49.3
1 mM $NaHCO_3$	17.3	9.6	-25.0
1 mM Na_2CO_3	19.6	10.8	-37.8
Sil-Co-Sil 75			
Nanopure	12.7	7.9	N/A
pH 7 Buffer	16.5	13.4	-29.4
pH 8 Buffer	18.6	15.8	-24.5
pH 9.6 Buffer	14.8	12.8	-45.4
pH 10 Buffer	15.3	13.6	-40.0
Alumina			
Nanopure	30.2	13.3	N/A
3 mM NaCl	31.2	11.5	36.0
0.1 mM $NaHCO_3$	40.2	24.3	12.0
1 mM $NaHCO_3$	37.1	18.5	-7.1
1 mM Na_2CO_3	26.6	12.9	-22.2
Alumina, unsettled after 60 minutes stagnation			
1 mM Na_2CO_3	4.1	2.5	-18.9

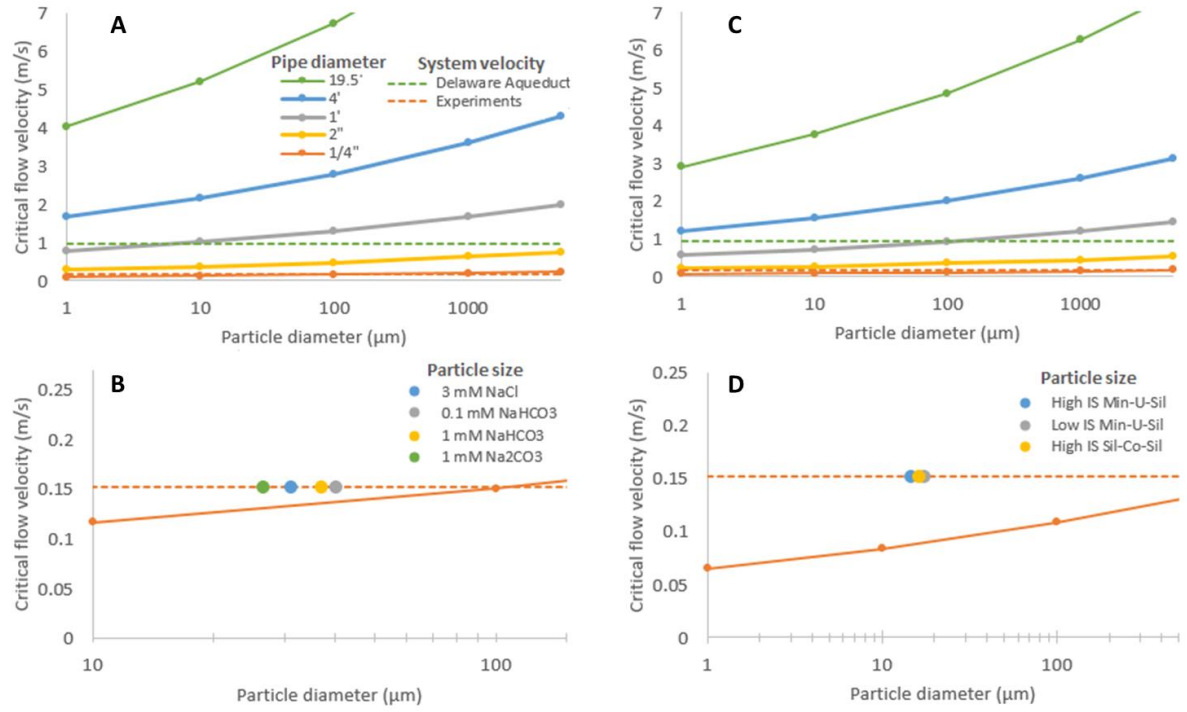

Figure 2-3 Critical settling velocity model: Critical settling velocities for particles in water at 20°C for A) alumina and C) silica in pipes of varying diameter, including real systems such as the Delaware Aqueduct (19.5') and these experiments (1/4"). Dotted lines are the flow velocities in those systems. Bottom graphs magnify the critical flow velocity scale to conditions relevant to this experiment. Dots represent B) mean alumina size in each low ionic strength solution and D) mean silica sizes in high ionic strength and high ionic strength solutions. However, visual observations indicated that the majority of the particles did settle to the bottom of the tubes despite the prediction herein, suggesting that the model approach would need to be adjusted to make accurate predictions in practice. The model in Danielson (2007) was calibrated for silica sand with mean diameters of 280-500 µm and tube diameter of 6.9 cm, which is outside the range in this experiment.

Leak Clogging with Silica

Both Min-U-Sil 40 and Sil-Co-Sil 75 in were shown to be capable of repairing leaks in nearly every solution, with the exception of Min-U-Sil 40 in the 1 mM $NaHCO_3$ solution (Table 2-3). None of the leaks repaired in the high ionic strength control after ten days. As noted before, there are similarities between the two types of silica; they have similar sizes and zeta potentials in the high ionic strength solutions (Table 2-2). Although both types of silica had similar particle characteristics in high ionic strength solutions, there was variation in clogging rate. For example,

Sil-Co-Sil 75 in the pH 9.6 buffer clogged all nine leaks over eight days, while Sil-Co-Sil 75 in pH 8 buffer only repaired one leak over ten days. Regardless of particle similarities, there seems to be some randomness in the length of time required to clog a leak with silica.

Table 2-3: Summary of Leak Clogging Results

Particle	Solution	Fraction repaired	Experiment duration (days)[1]
N/A	Control	0/9	10
Min-U-Sil 40	pH 7 Buffer	4/8	10
	pH 8 Buffer	5/9	10
	pH 9.6 Buffer	4/9	10
	pH 10 Buffer	8/9	10
	3 mM NaCl	9/9	8
	0.1 mM $NaHCO_3$	6/9	10
	1 mM $NaHCO_3$	0/9	10
	1 mM Na_2CO_3	6/9	10
Sil-Co-Sil 75	pH 7 Buffer	4/9	10
	pH 8 Buffer	1/9	10
	pH 9.6 Buffer	9/9	8
	pH 10 Buffer	5/9	10
Alumina	3 mM NaCl	9/9	4
	0.1 mM $NaHCO_3$	8/8	3
	1 mM $NaHCO_3$	4/9	10
	1 mM Na_2CO_3	6/9	10
Alumina, unsettled after 60 min. stagnation	1 mM Na_2CO_3	1/9	10

[1]Experiments were run for 10 days but were ended early if every leaked was clogged.

Leak Clogging with Alumina

The results of the leak clogging experiments with alumina particles provide valuable insight into the effects of water quality on repair efficiency. Like silica, alumina was shown capable of leak clogging in each solution (Table 2-3), though alumina was added at higher concentration. The two alumina solutions that clogged all of the leaks were 3 mM NaCl and 0.1 mM $NaHCO_3$. While their sizes were significantly different, the zeta potential of alumina in both of these solutions was positive while the borosilicate capillaries should have a negative charge (Lameiras et al., 2008). This suggests that opposite charges on the particle and leak surfaces could be highly conducive to initiating processes of leak clogging, as the particles quickly adhere over and inside the leak as a monolayer. This also promotes the notion that smaller particles whose charge is opposite of that

in the leak may be more effective in repairing leaks because they have lower tendency to settle out in the system. On the other hand, there is homogeneity in the materials in real pipe systems outside of this experiment, and the particles should also deposit to pipe surfaces other than the inside of the leak and be more rapidly lost from the system.

Turbidity was tracked in the recirculation systems for each solution over 24 hours (Figure 2-4). However, turbidity is not exactly proportional to particle volume as it can depend on particle size (Baker and Lavelle, 1984; Gibbs and Wolanski, 1992). For the alumina size ranges in these experiments (>0.5 μm), the turbidity should decrease as particles grow larger, assuming equal particle volumes (Morris, 1987). Because the alumina in the 0.1 mM $NaHCO_3$ and 1 mM $NaHCO_3$ solutions has higher average size, there is a lower amount of turbidity generated in those solutions per unit volume of alumina particles.

There is a rapid drop in turbidity in every system in the first hour after the water is replaced, likely due to particles settling out of the system (Figure 2-4). While the flow velocity is fast enough to keep the mean particle size suspended (Figure 2-3), there are alumina particles that are large enough (>100 μm) to settle out in each system (Figure 2-5). The portions of each recirculation system where particle build-up occurred include the pressure gauge, valve, pressure tank, and 90° elbows. These components likely contributed to the initial turbidity drop. The area under the curves in Figure 2-4A was calculated to estimate the relative volume of alumina particles that were flowing through each system (Figure 2-4B). 3 mM NaCl, 0.1 mM $NaHCO_3$, and 1 mM $NaHCO_3$ solutions had similar total turbidities over 24 hours, while 1 mM Na_2CO_3 had the highest total turbidity. Although the 1 mM Na_2CO_3 experiment had the highest overall turbidity pass through it each day, it did not fully repair. This contradicts previous studies showing that pore clogging rate depends on the number of particles that pass through the pore (Wyss et al., 2006). Furthermore, the condition with the second highest turbidity had the lowest repair rate after 10 days. These findings support our previous assertion that particle charge is a dominant factor in repair.

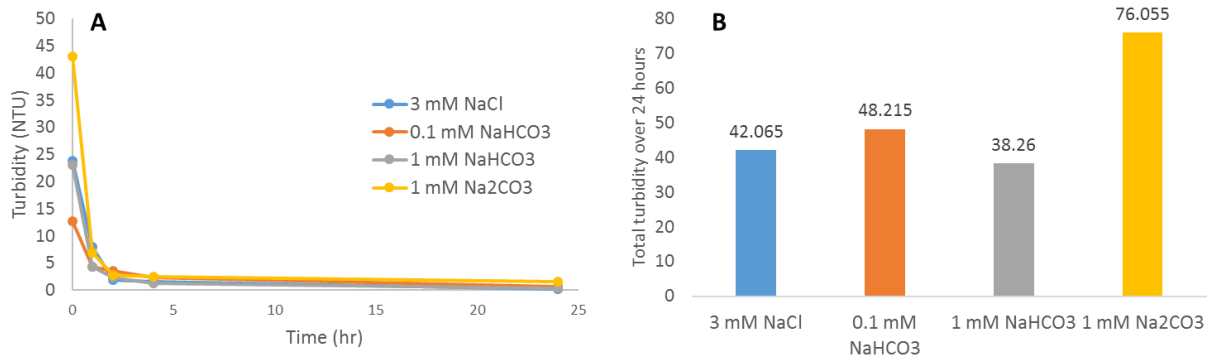

Figure 2-4 Alumina turbidity measurements: A) Turbidity of alumina solutions passing through the recirculation systems over a 24-hour period. B) Area under each curve in Figure 2-4A, proportional to the total amount of particles that pass through each system over 24 hours.

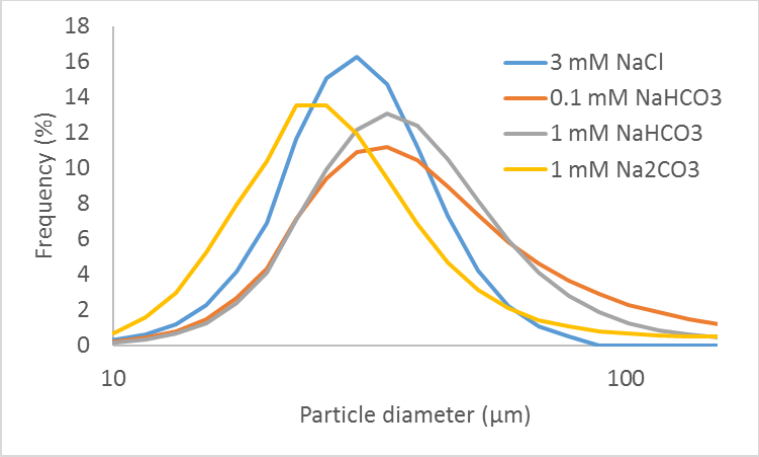

Figure 2-5 Particle size distributions of alumina particles.

A leak clogging experiment on the suspension of smaller alumina particles that did not settle after 60 minutes of stagnation was done to assess leak repair in a system that retains most of its initial turbidity. 60 minutes was selected as the stagnation time because more than 50% the initial turbidity was still suspended in the recirculation system after running for 24 hours (Figure 2-6). While two leaks were temporarily clogged for one and four days, only one leak was clogged after ten days (Table 2-3). The phenomenon of temporary leak clogging before becoming unclogged occurred in the other experiments as well. Additional experiments in 3 mM NaCl or 0.1 mM $NaHCO_3$ solutions could be performed to test if the unsettled particles have a higher clogging efficiency with a positive zeta potential.

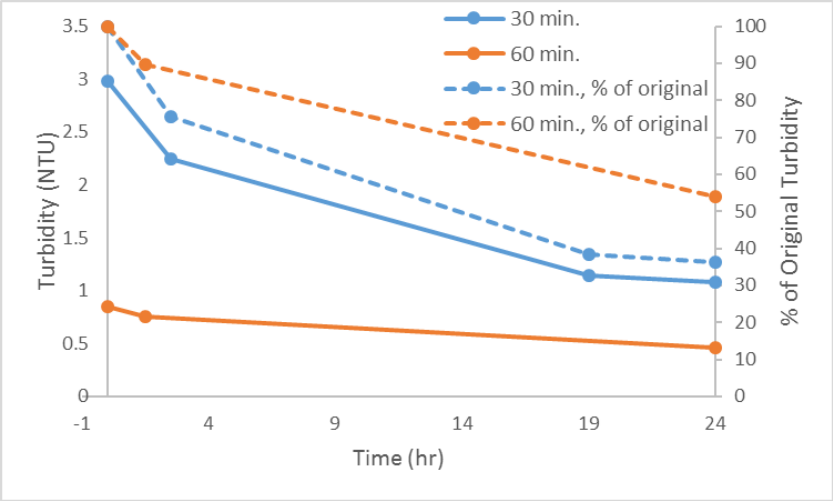

Figure 2-6 Unsettled alumina turbidity over 24 hours.

The final disposition of particles in holes that were successfully clogged also varied widely (Figure 2-7). For example, microscope images observe build-up of smaller particles over a leak (Figure 2-7B), clogging by a single large particle (Figure 2-7C), and clogging by small particles further down the path of the leak (Figure 2-7D). The wall thickness of the pipe material could be an important factor in repair via particle clogging. For example, particles traveling through leaks in pipes with lower wall thickness will have less opportunities to collide with and stick to the leak wall than particles traveling through leaks in pipes with greater wall thickness.

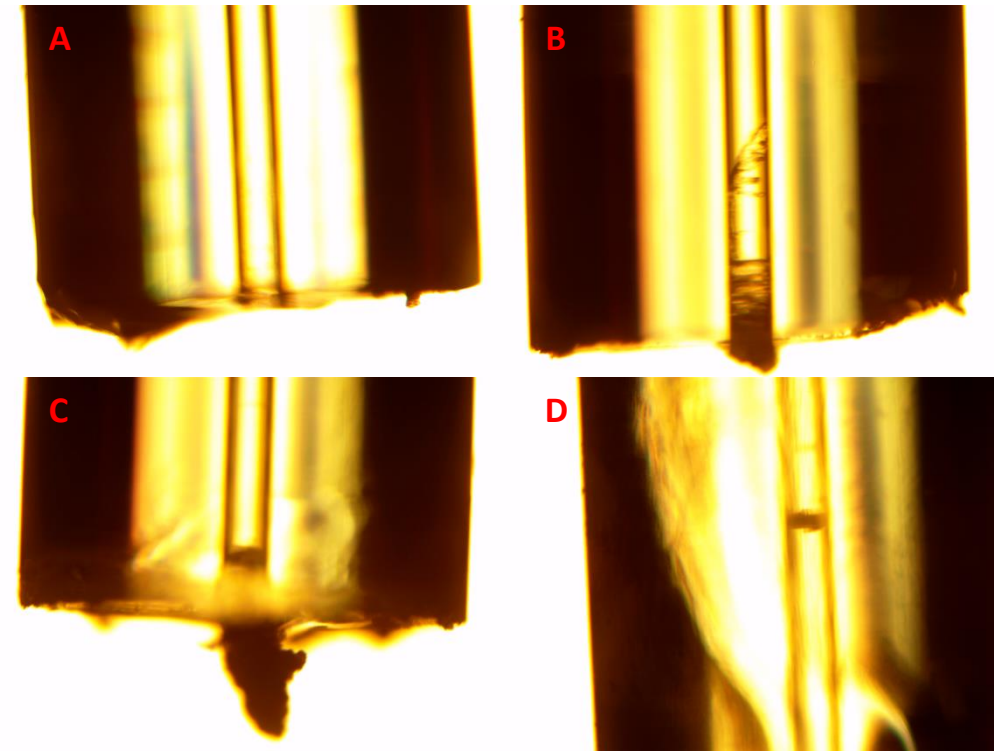

Figure 2-7: Microscope images of clogged capillaries. 40x magnification of 250 μm i.d. capillaries from -alumina in 1 mM $NaHCO_3$ clogging experiment. A) Non-repaired leak. B) Potential leak repair by gradual build-up of particles. The clog extends approximately 600 μm into the leak. C) Leak repaired by a single large particle. D) Leak repaired further down the leak path.

2.4 Conclusions

Analysis of particle sizes, zeta potential, and leak clogging data from silica and alumina particles in various solutions yielded the following conclusions:

- Changing water quality impacted the size of alumina particles, but not silica particles. Alumina sizes were consistent with expectations based on their zeta potential. Silica particles were roughly the same size likely because they had highly negative zeta potentials.
- Silica particles were proven capable of repairing leaks in high and low ionic strength solutions, but the water quality was not shown to influence leak clogging rate.
- Water quality has a pronounced impact on clogging with alumina particles. Alumina with positive zeta potential repaired significantly faster than alumina with negative zeta

potential. This could be due to the opposite surface charges between the negatively charged capillary and positively charged alumina.

- The total turbidity of alumina particles that passes through a leak does not affect its clogging rate. The experiment that had the highest estimated volume of alumina particles repaired relatively slow.
- Smaller alumina particles (i.e. alumina particles that do not settle out of the solution) were ineffective at clogging leaks even though they remained suspended in solution over longer periods of time. In a real system, leaks that are far from the point of particle addition are unexpected to repair as fast as leaks close to the point of particle addition.

2.5 Limitations and Future Research

While these particle clogging experiments demonstrate a proof of concept, there are several limitations in this work that prevent it from being applied to distribution systems. The pipe diameter in these experiments is orders of magnitude lower than actual water mains. Models predict that the critical flow velocity is strongly dependent on pipe diameter and particles will settle more frequently in pipes with larger diameters (Soepyan et al., 2013). Distribution systems also operate at higher pressures, typically around 120 psi. It is possible that the clogs in these experiments at 20 psi would not hold under higher pressure. Leak geometry in distribution systems is also different, as longitudinal cracks are more prominent than the pinhole leaks simulated in these experiments. Finally, water hammering, which is a surge in system pressure that results from valve closure, occurs in practice. Sudden spikes in pressure could unclog leaks while turbulent flow conditions during hammering events can suspend settled particles in the system.

Both steps in the two-step model have been confirmed as being important for leak clogging. Two extremes were tested with regard to particle transport and particle clogging. Larger particles settled relatively fast but were more capable of clogging leaks, and smaller particles stayed suspended but were less capable of clogging leaks. Future research should determine how far along a pipe leaks can be effectively repaired. There should exist an optimal particle size that is capable of flowing to and repairing leaks further from the point of particle addition. Methods of transporting larger particles greater distances should also be considered, such as temporary increases in flow velocity. The critical flow velocity model formulated in Danielson (2007) needs to be calibrated to the

conditions in these experiments as well as the conditions relevant to water distributions systems. Modeling critical flow velocity in a real system can have benefits outside of autogenous repair. For example, presence of lead particulates is a concern in some systems (Masters et al., 2016) and having accurate models for critical flow velocity would allow for tracking its transport.

2.6 References

Agbangla, G.C., Climent, É., and Bacchin, P. (2012). Experimental investigation of pore clogging by microparticles: Evidence for a critical flux density of particle yielding arches and deposits. *Separation and Purification Technology*. 101, 42.

American Society of Civil Engineers (ASCE). (2013). *2013 Report Card for America's Infrastructure*. Reston, VA: ASCE. Available at: http://www.infrastructurereportcard.org/a/#p/drinking-water/conditions-and-capacity

American Water Works Association Research Foundation (AWWARF). (2001). *Pathogen Intrusion into the Distribution System*. Denver, CO: AWWA.

Baker, E.T. and Lavelle, J.W. (1984). The effect of particle size on the light attenuation coefficients of natural suspensions. *Journal of Geophysical Research*. 89, 8197.

Cabrejos, F.J. and Klinzing, G.E. (1994). Pickup and saltation mechanisms of solid particles in horizontal pneumatic transport. *Powder Technology*. 79, 173.

Center for Neighborhood Technology (CNT). (2013). *The Case for Fixing Leaks: Protecting people and saving water while supporting economic growth in the Great Lakes region*. Chicago, IL: Center for Neighborhood Technology.

Danielson, T.J. (2007). Sand transport modelling in multiphase pipelines. Presented at the *2007 Offshore Technology Conference*, Houston, Texas, USA, April 30 – May 3.

Dersoir, B., Robert de Saint Vincent, M., Abkarian, M., and Tabuteau, H. (2015). Clogging of a single pore by colloidal particles. *Microfluid Nanofluid.* 19, 953.

Edvardsen, C. (1999). Water permeability and autogenous healing of cracks in concrete. *ACI Materials Journal*. 96, 448.

Gibbs, R.J. and Wolanski, E. (1992). The effect of flocs on optical backscattering measurements of suspended material concentration. *Marine Geology*. 107, 289.

Hajra, M.G., Reddi, L.N., Glasgow, L.A., Xiao, M., and Lee, I.M. (2002). Effects of ionic strength on fine particle clogging of soil filters. *Journal of Geotechnical and Geoenvironmental Engineering*. 128, 631.

Lameiras, F.S., Leles de Souza, A., Rodrigues de Melo, V.A., Nunes, E.H.M., and Braga, I.D. (2008). Measurement of the zeta potential of planar surfaces with a rotating disk. *Materials Research*. 11, 217.

Masters, S., Welter, G.J., and Edwards, M. (2016). Seasonal variations in lead release to potable water. *Environmental Science and Technology*.

Morris, T.M. (1987). The relationship between haze and the size of particles in beer. *Journal of the Institute of Brewing*. 93, 13.

Mustin, B. and Stoeber, B. (2010). Deposition of particles from polydisperse suspensions in microfluidic systems. *Microfluid Nanofluid*. 9, 905.

Parks, J., Edwards, M, Vikesland, P., and Dudi, A. (2010). Effects of bulk water chemistry on autogenous healing of concrete. *Journal of Materials in Civil Engineering*. 22, 515.

Schwarz, J.A., Driscoll, C.T., and Bhanot, A.K. (1984). The zero point of charge of silica-alumina oxide suspensions. *Journal of Colloid and Interface Science*. 97, 55.

Shanaghan, P.E. (2012). Assessing drinking water infrastructure need. *Journal of the American Water Works Association*. 104, 14.

Soepyan, F.B., Cremaschi, S., Sarica, C., Subramani, H.J., and Kouba G.E. (2013). Solids transport models comparison and fine-tuning for horizontal, low concentration flow in single-phase carrier fluid. *AIChE Journal*. 60, 76.

Tang, M., Triantafyllidou, S., and Edwards, M. (2013). *In situ* remediation of leaks in potable water supply systems. *Corrosion Reviews*. 31, 105.

Tang, M., Triantafyllidou, S., and Edwards, M. (2015). Autogenous metallic pipe leak repair in potable water systems. *Environmental Science and Technology*. 49, 8697.

Thomas, A.D. (1979). Predicting the deposit velocity for horizontal turbulent pipe flow of slurries. *International Journal of Multiphase Flow*. 5, 113.

Turian, R.M., Hsu, F.L., and Ma, T.W. (1987). Estimation of the critical velocity in pipeline flow of slurries. *Powder Technology*. 51, 35.

Walski, T.M. and Lutes, T.L. (1994). Hydraulic transients cause low pressure problems. *Journal of the American Water Works Association*. 86, 24.

Wyss, H.M. Blair, D.L., Morris, J.F., Stone, H.A., and Weitz, D.A. (2006). Mechanism for clogging or micro-channels. *Physical Review E*. 74, 1.

Appendix: Supporting Tables and Figures

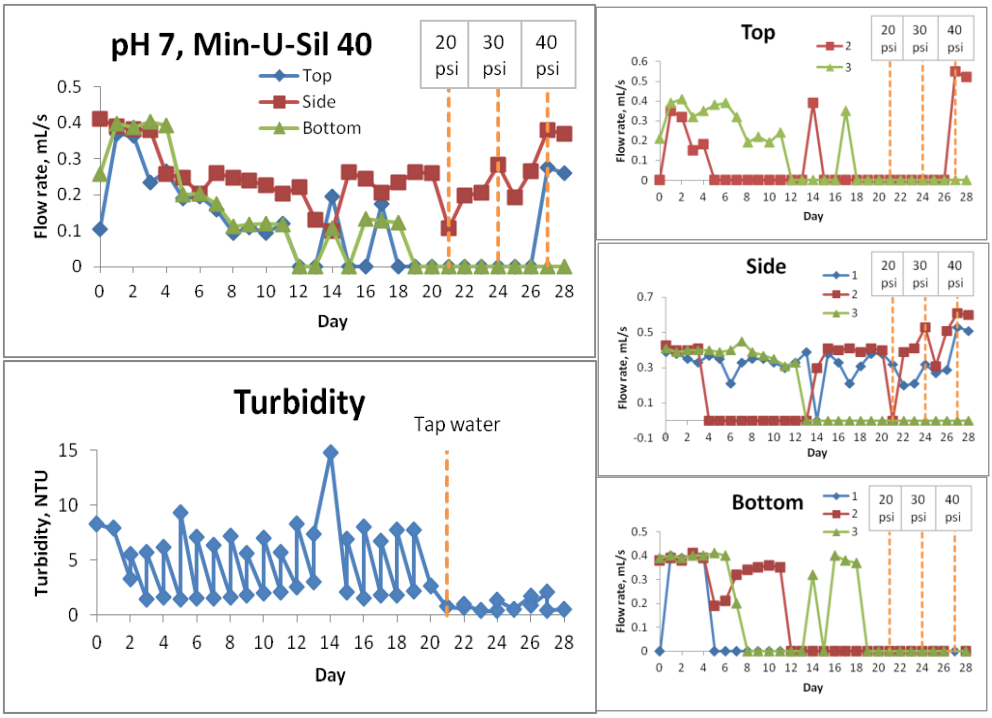

Figure A-1: Leak clogging and turbidity results for Min-U-Sil 40 in pH 7 buffer

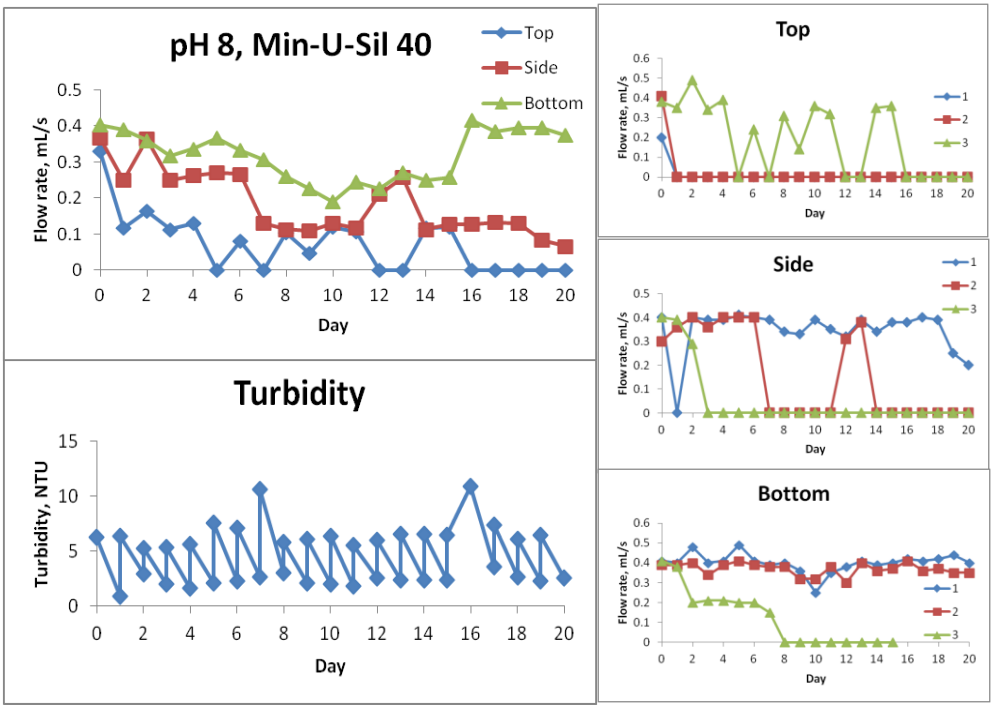

Figure A-2: Leak clogging and turbidity results for Min-U-Sil 40 in pH 8 buffer

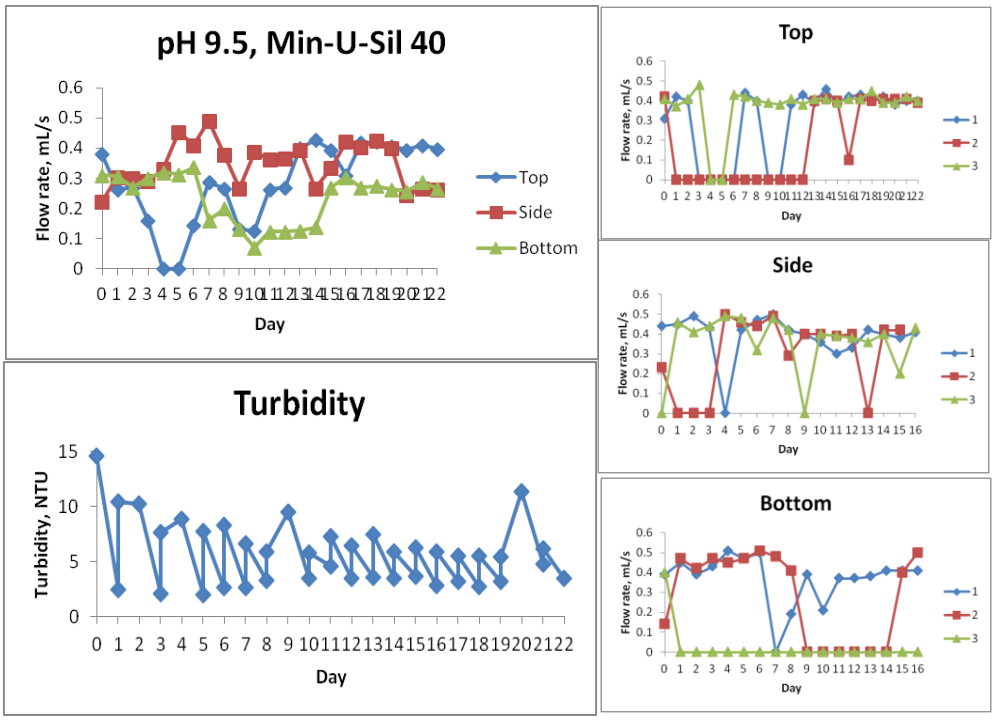

Figure A-3: Leak clogging and turbidity results for Min-U-Sil 40 in pH 9.6 buffer

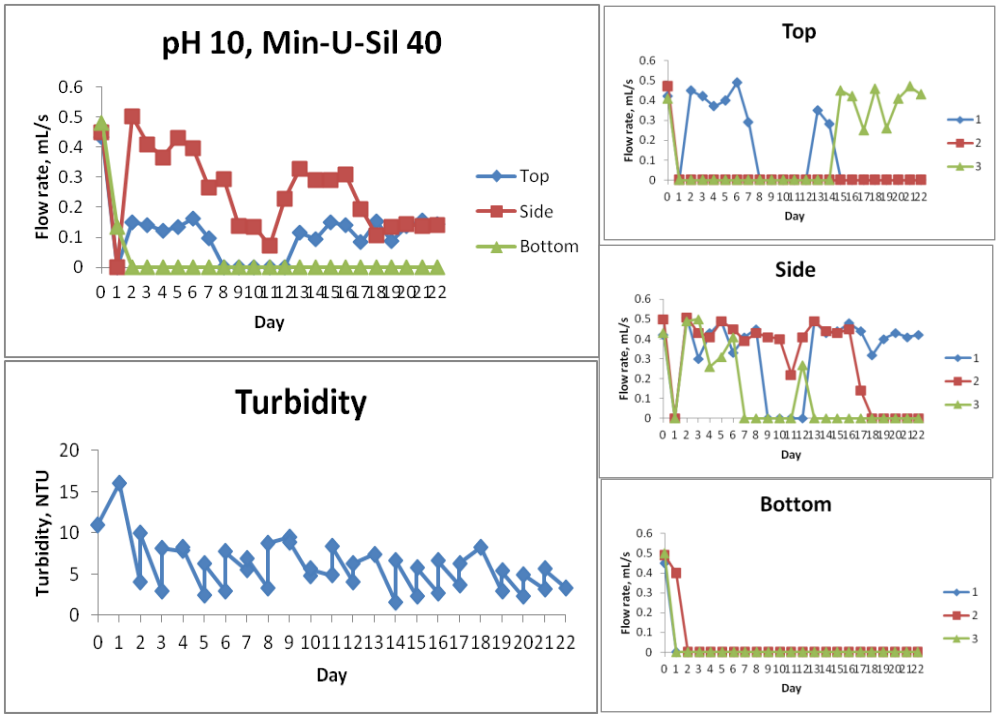

Figure A-4: Leak clogging and turbidity results for Min-U-Sil 40 in pH 10 buffer

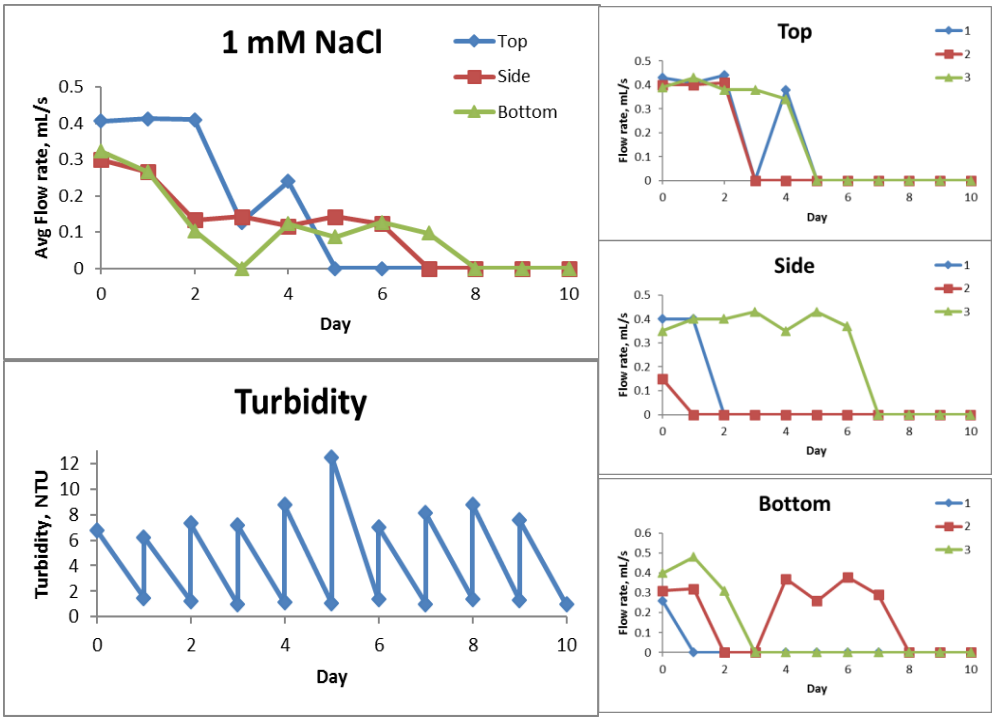

Figure A-5: Leak clogging and turbidity results for Min-U-Sil 40 in 3 mM NaCl solution

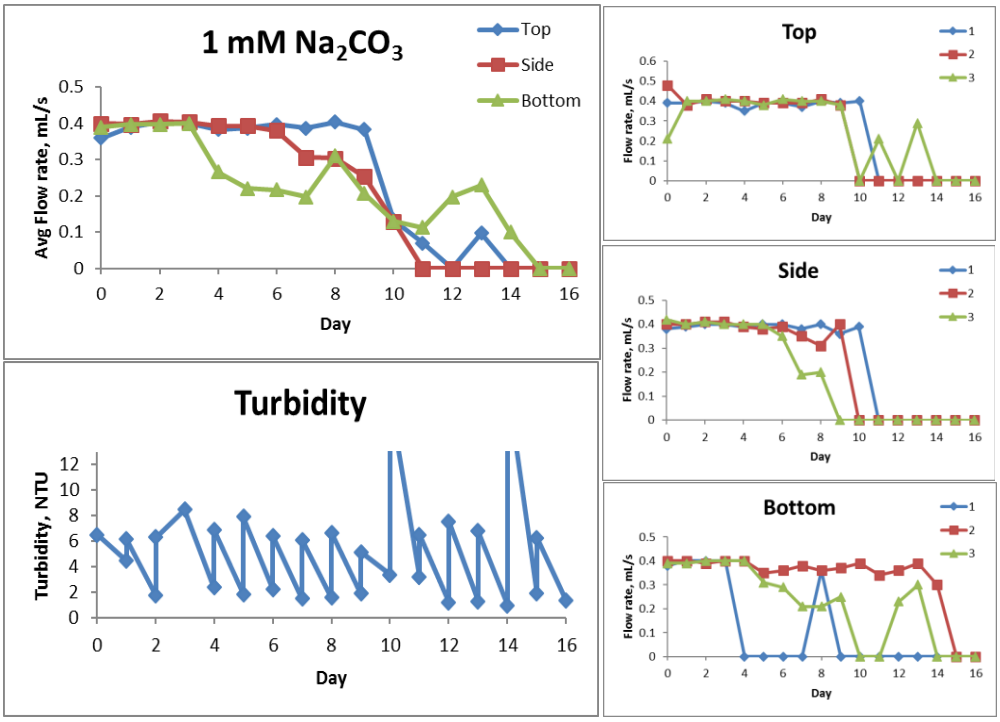

Figure A-6: Leak clogging and turbidity results for Min-U-Sil 40 in 1 mM Na_2CO_3 solution

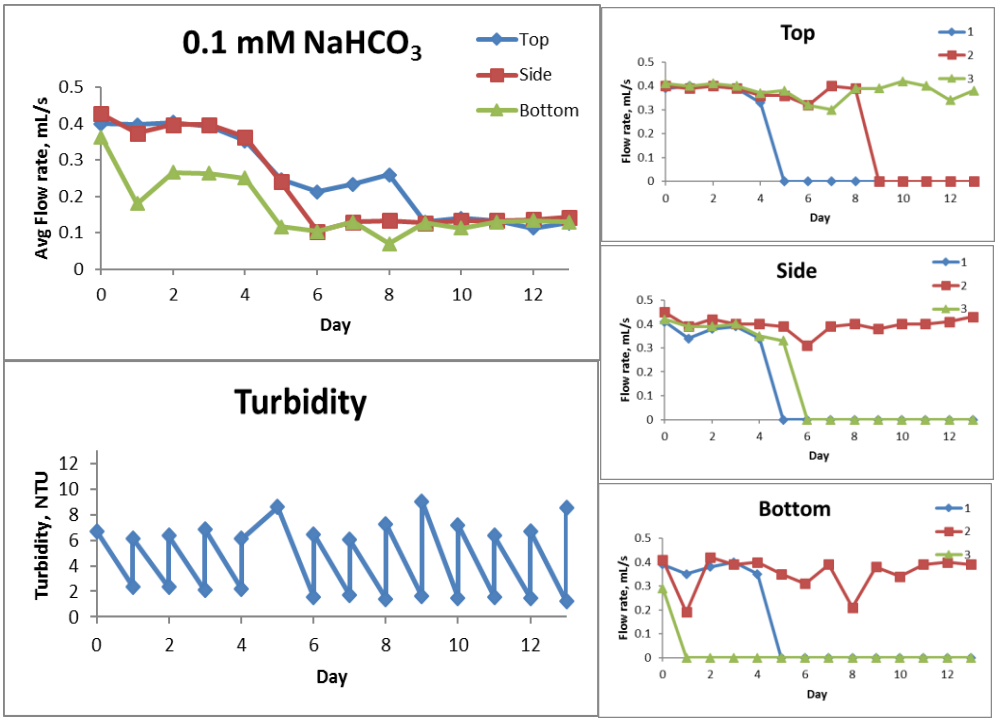

Figure A-7: Leak clogging and turbidity results for Min-U-Sil 40 in 0.1 mM $NaHCO_3$ solution

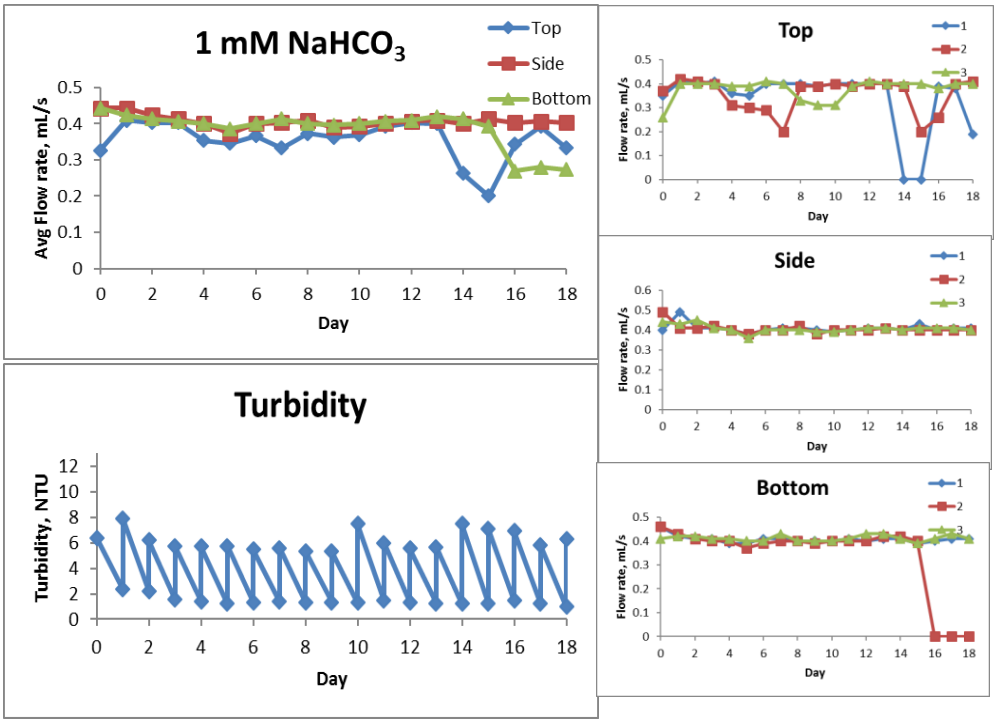

Figure A-8: Leak clogging and turbidity results for Min-U-Sil 40 in 1 mM $NaHCO_3$ solution

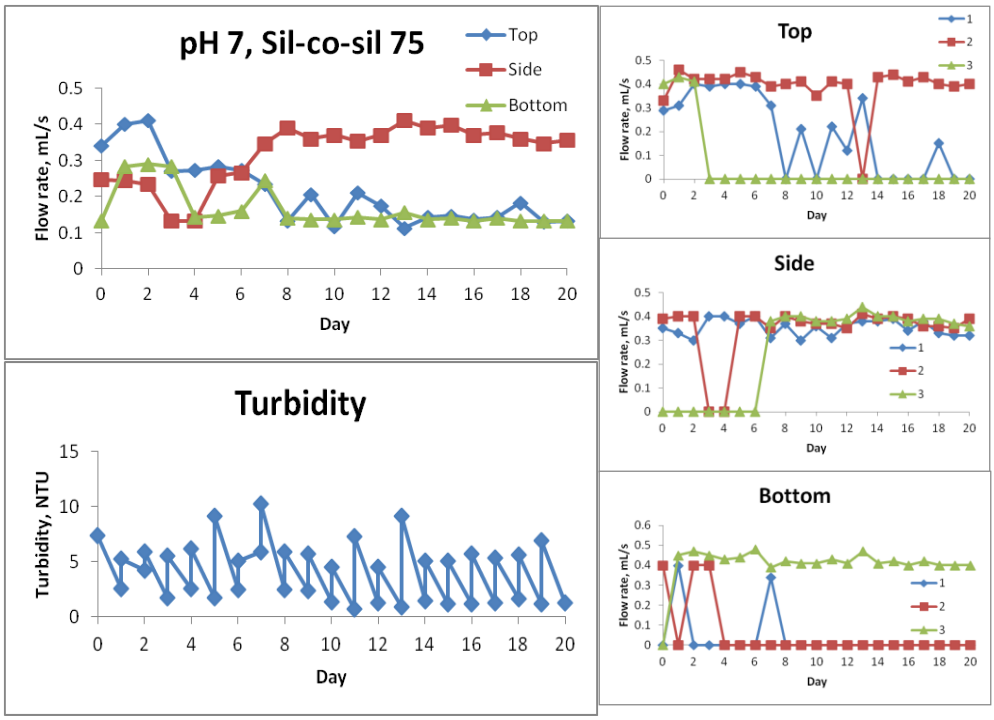

Figure A-9: Leak clogging and turbidity results for Sil-Co-Sil 75 in pH 7 buffer solution

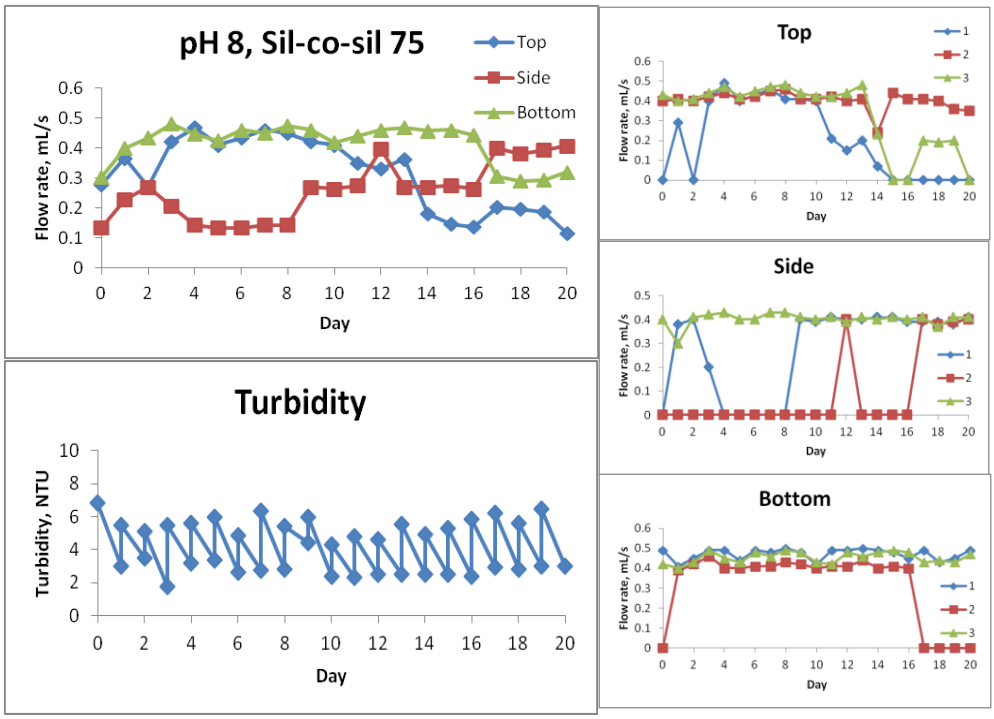

Figure A-10: Leak clogging and turbidity results for Sil-Co-Sil 75 in pH 8 buffer solution

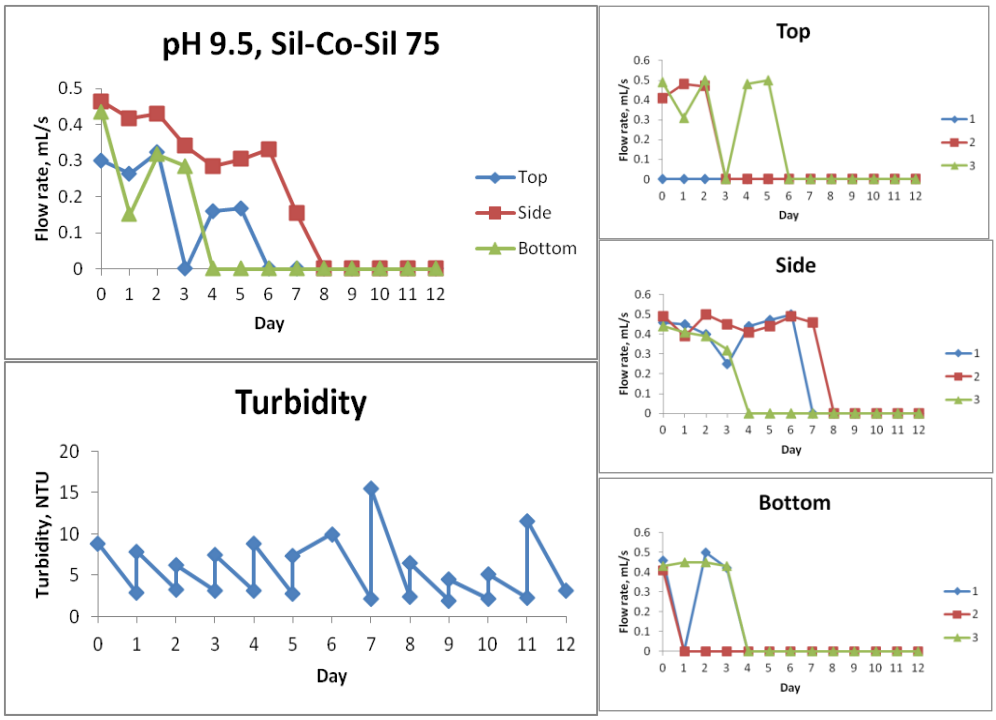

Figure A-11: Leak clogging and turbidity results for Sil-Co-Sil 75 in pH 9.6 buffer solution

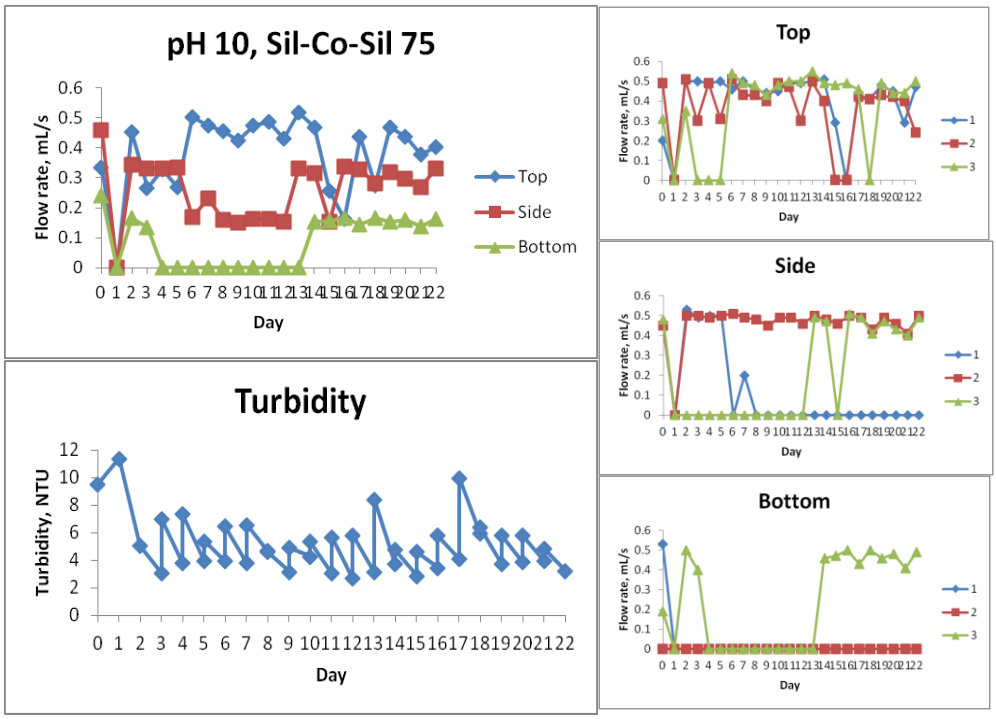

Figure A-12: Leak clogging and turbidity results for Sil-Co-Sil 75 in pH 10 buffer solution

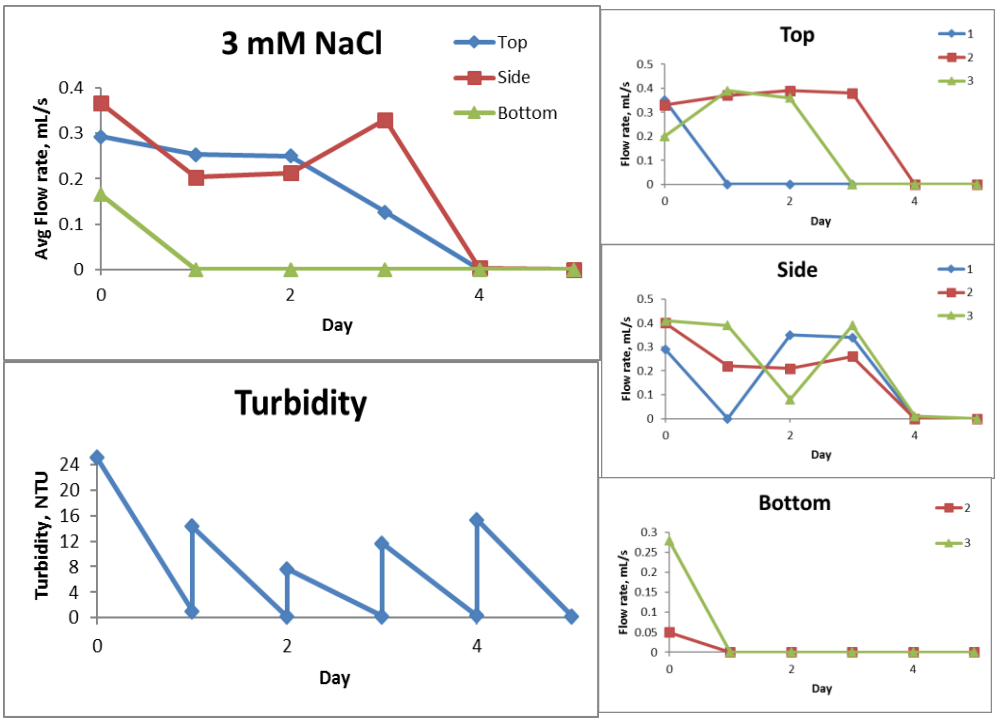

Figure A-13: Leak clogging and turbidity results for alumina in 3 mM NaCl solution

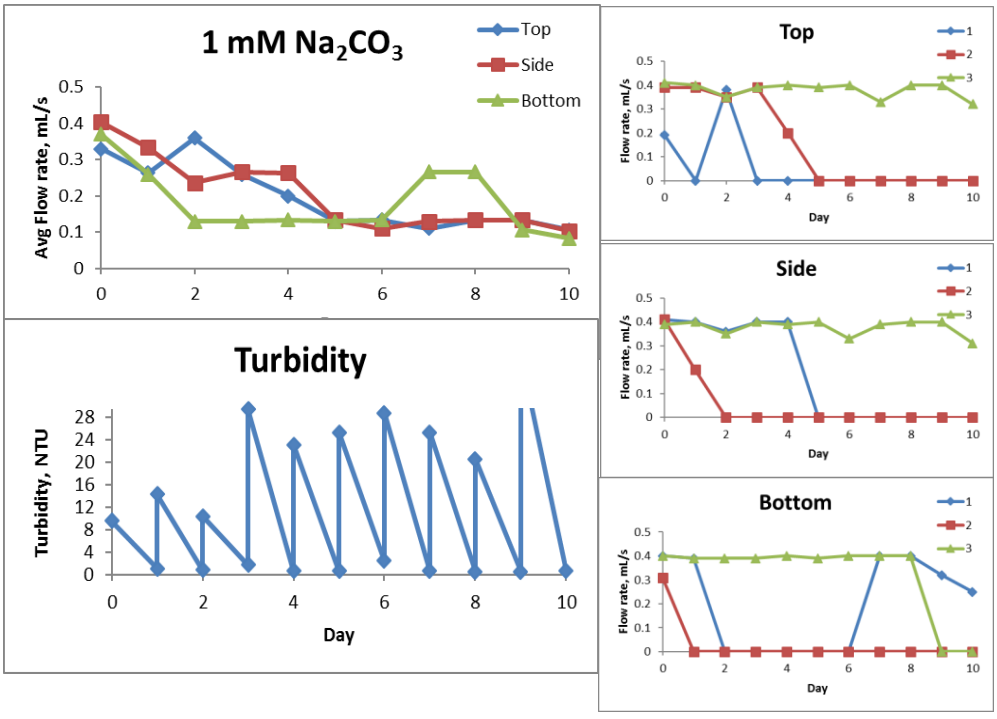

Figure A-14: Leak clogging and turbidity results for alumina in 1 mM Na_2CO_3 solution

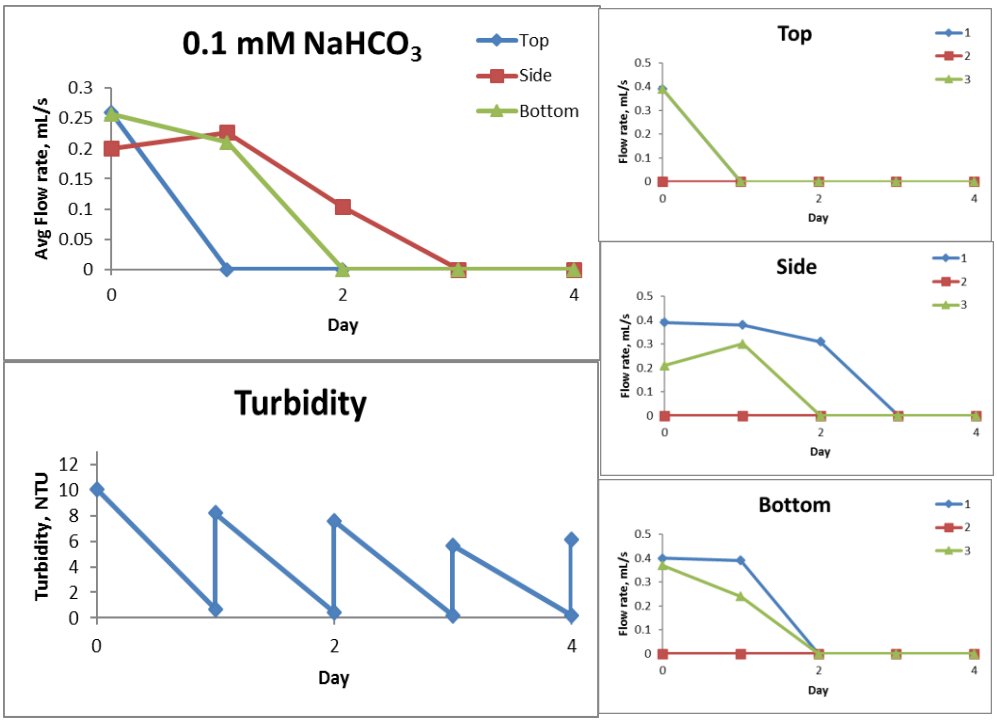

Figure A-15: Leak clogging and turbidity results for alumina in 0.1 mM $NaHCO_3$ solution

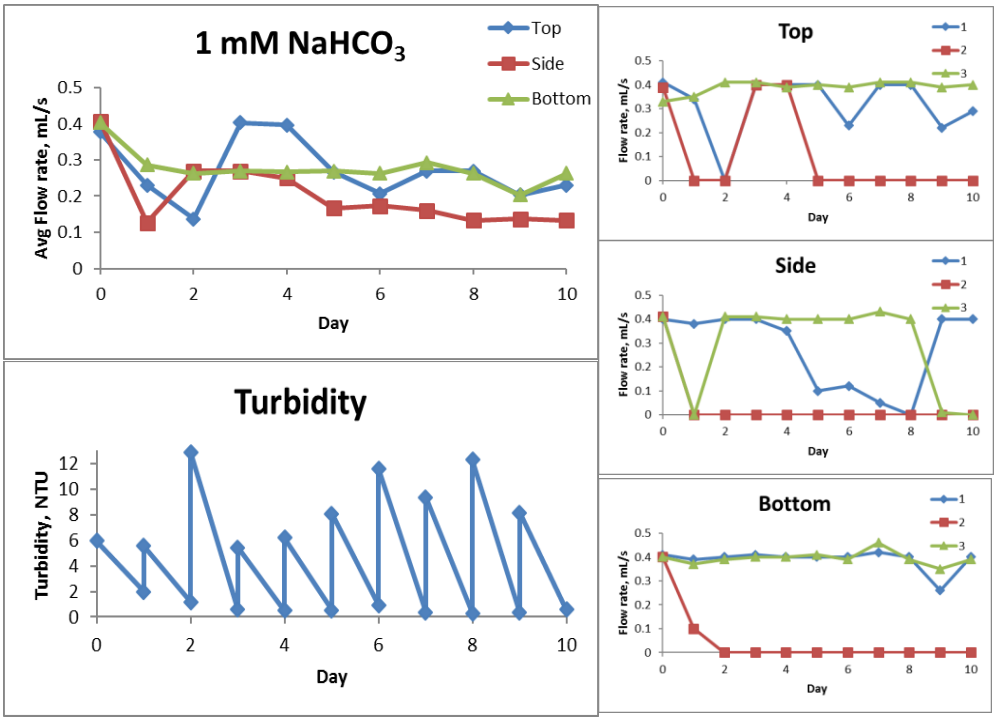

Figure A-16: Leak clogging and turbidity results for alumina in 1 mM $NaHCO_3$ solution

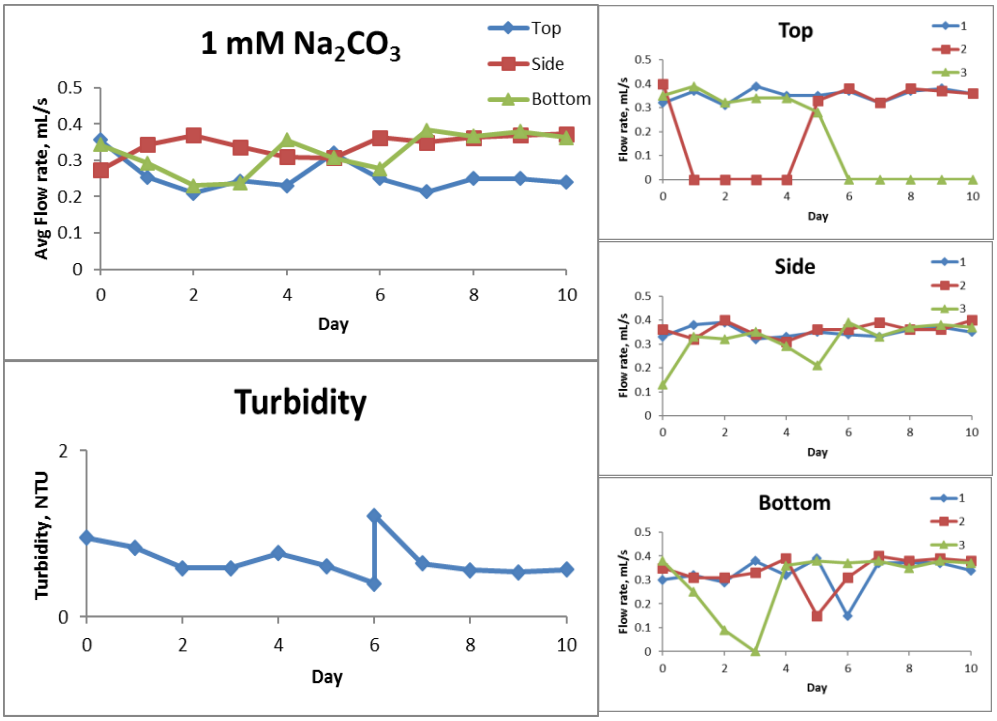

Figure A-17: Leak clogging and turbidity results for unsettled alumina in 1 mM Na_2CO_3 solution

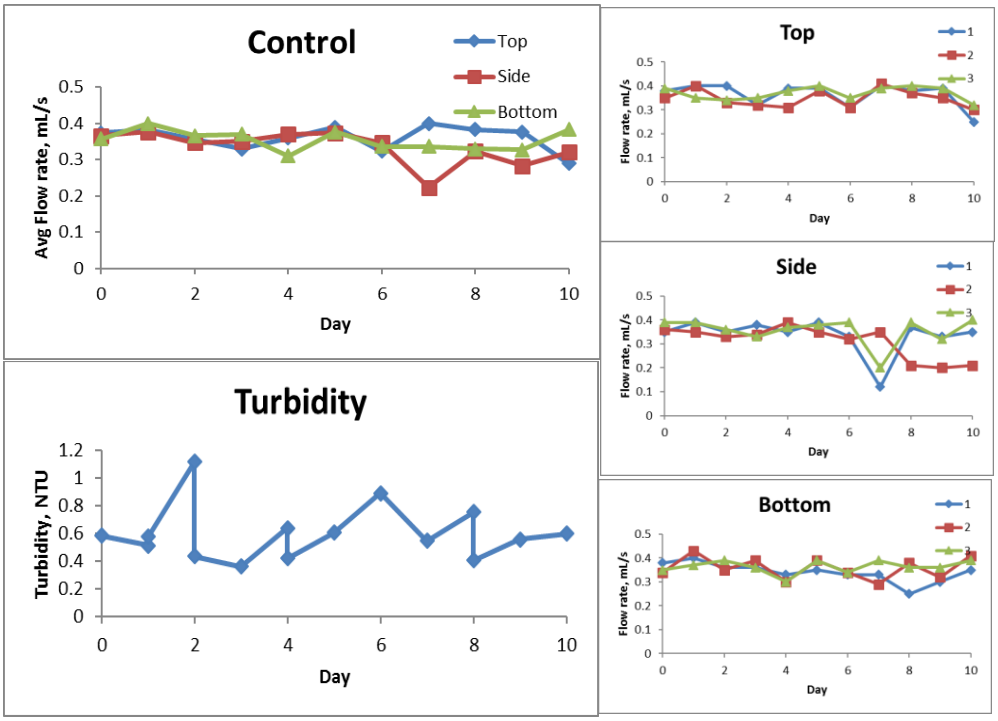

Figure A-18: Leak clogging and turbidity results for unsettled alumina in control solution

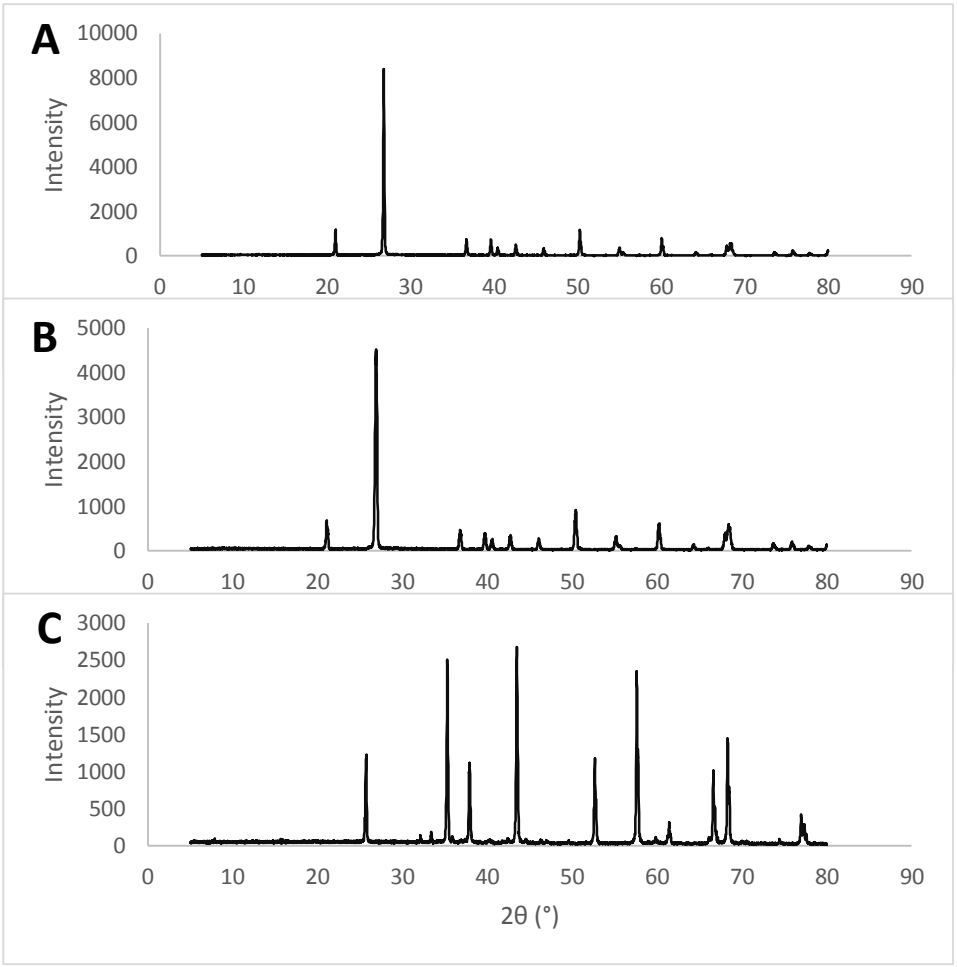

Figure A-19: XRD results for A) Min-U-Sil 40, B) Sil-Co-Sil 75, and C) alumina

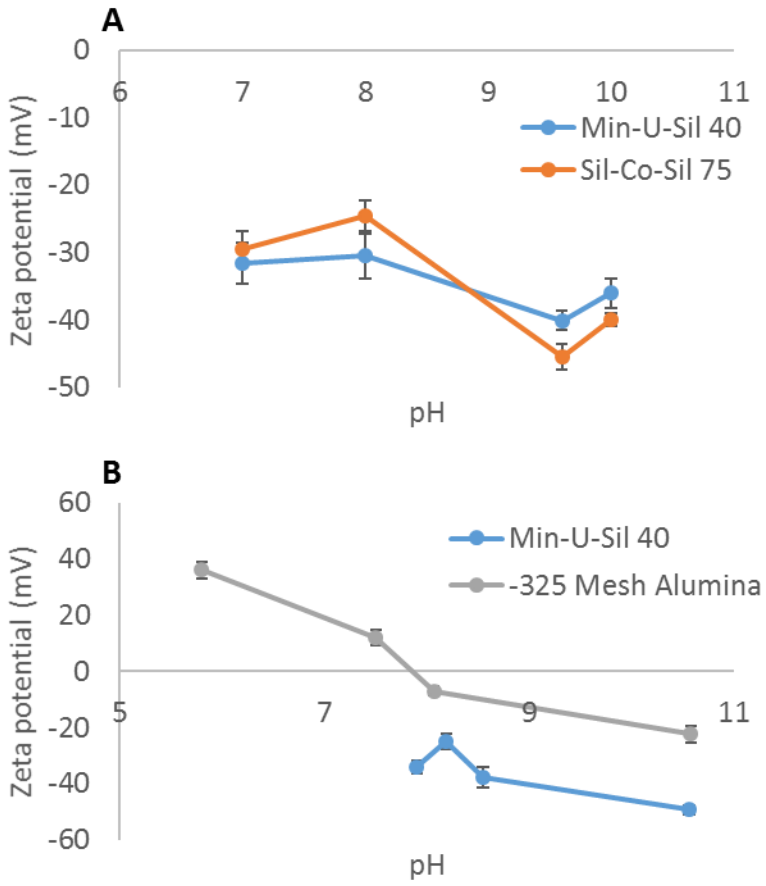

Figure A-20: Zeta potential measurements for A) high ionic strength and B) low ionic strengths solutions. Error bars represent 95% confidence interval

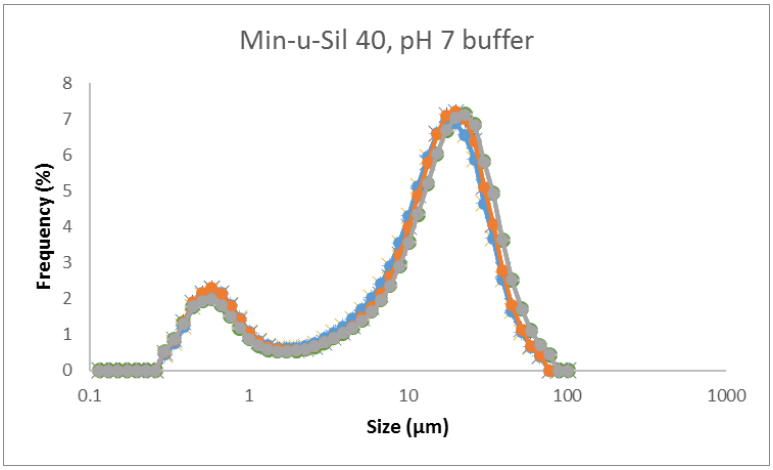

Figure A-21: Min-U-Sil 40 particle size distribution in pH 7 buffer solution

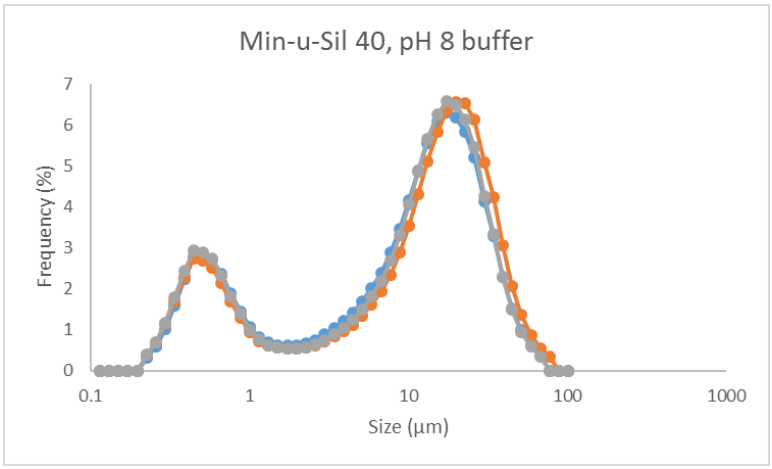

Figure A-22: Min-U-Sil 40 particle size distribution in pH 8 buffer solution

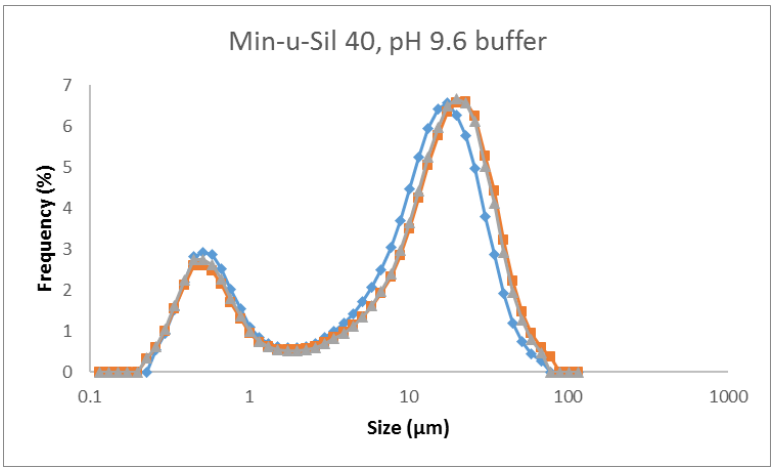

Figure A-23: Min-U-Sil 40 particle size distribution in pH 9.6 buffer solution

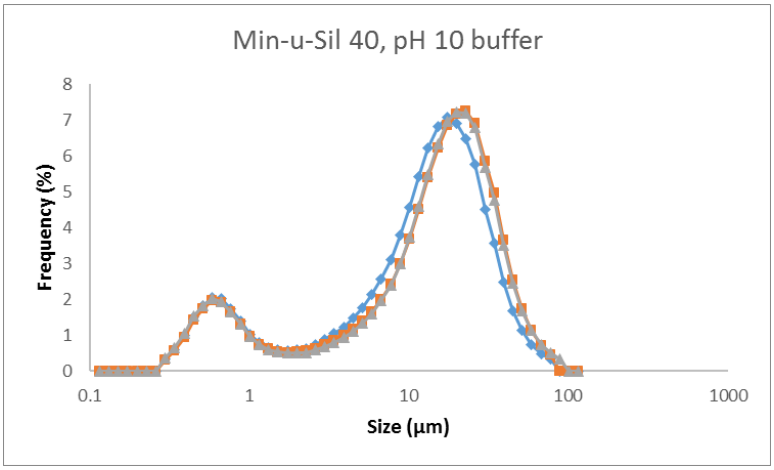

Figure A-24: Min-U-Sil 40 particle size distribution in pH 10 buffer solution

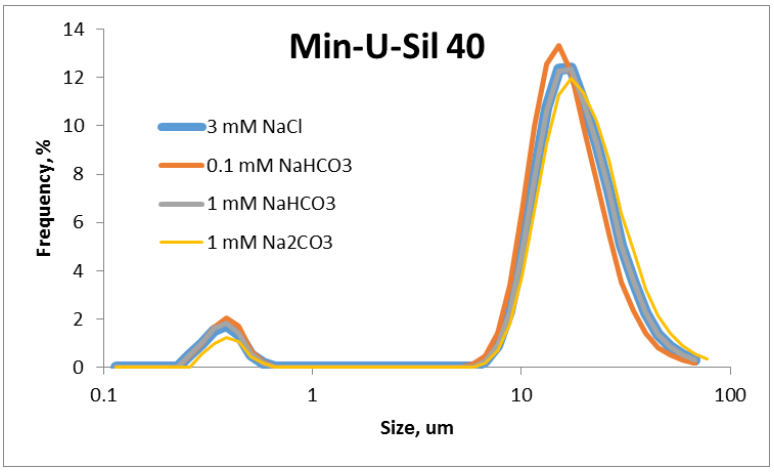

Figure A-25: Min-U-Sil 40 particle size distribution in low ionic strength solutions

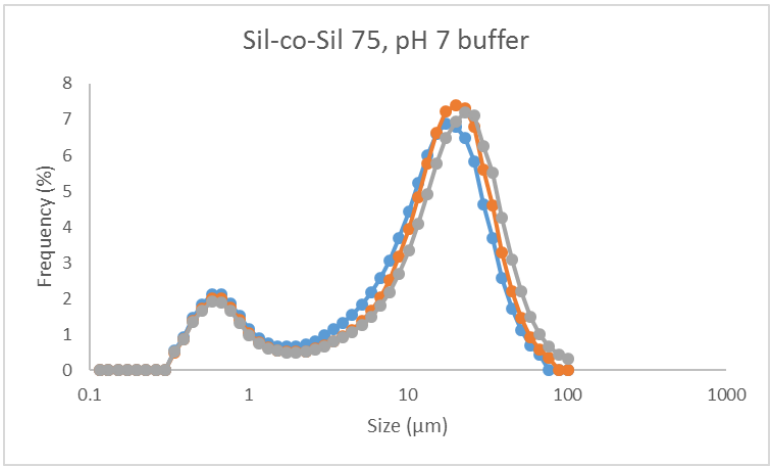

Figure A-26: Sil-Co-Sil 75 particle size distribution in pH 7 buffer solution

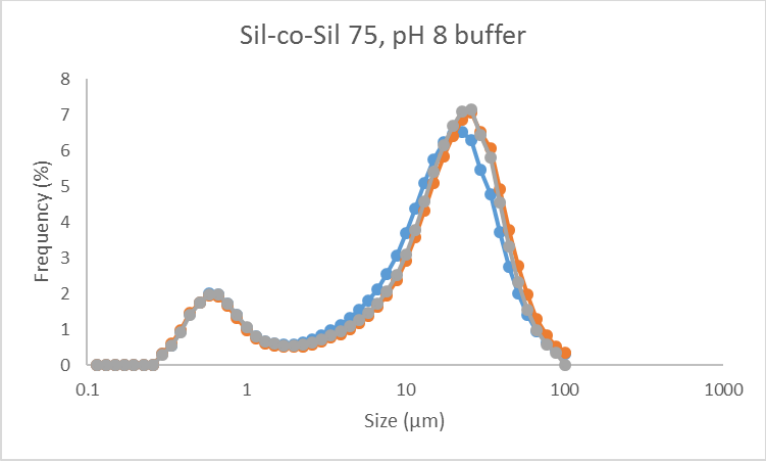

Figure A-27: Sil-Co-Sil 75 particle size distribution in pH 8 buffer solution

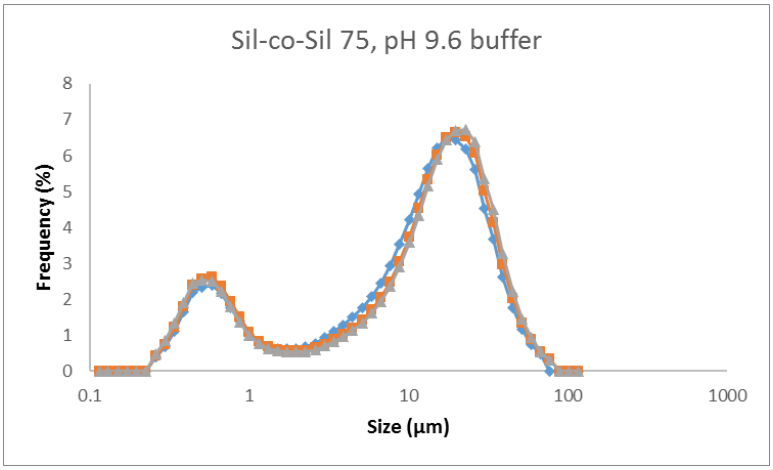

Figure A-28: Sil-Co-Sil 75 particle size distribution in pH 9.6 buffer solution

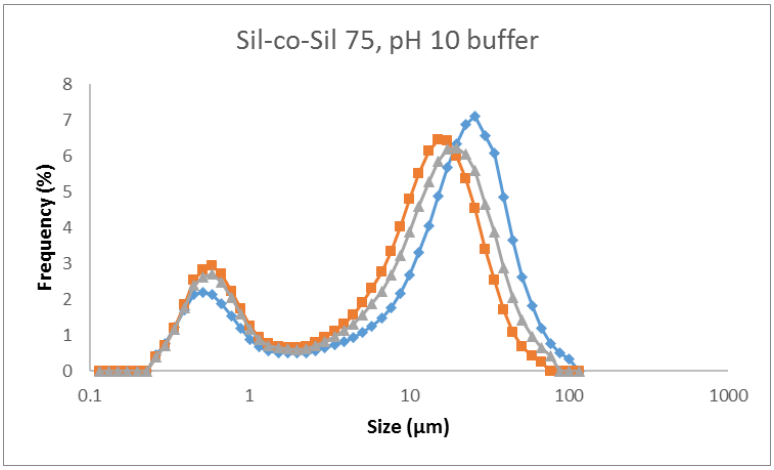

Figure A-29: Sil-Co-Sil 75 particle size distribution in pH 10 buffer solution

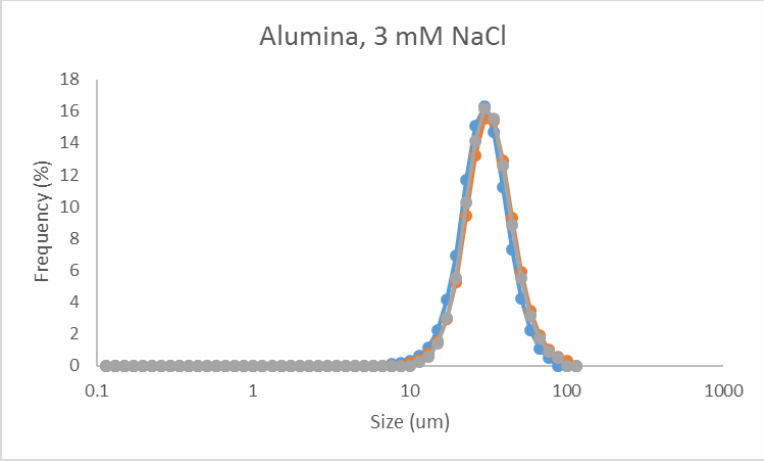

Figure A-30: Alumina particle size distribution in 3 mM NaCl solution

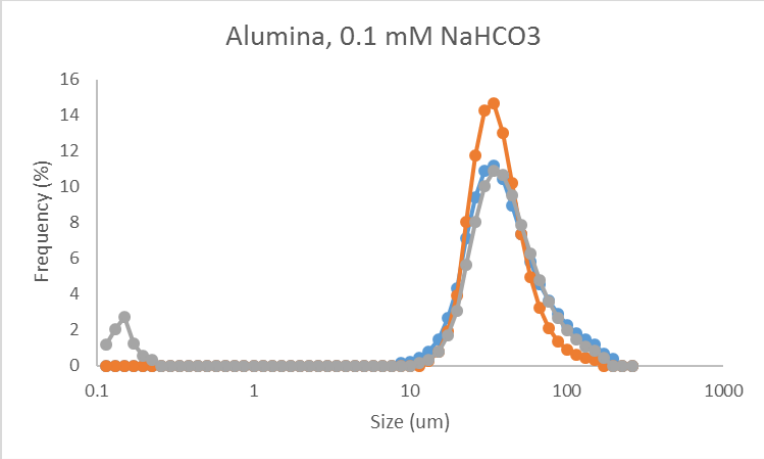

Figure A-31: Alumina particle size distribution in 0.1 mM $NaHCO_3$ solution

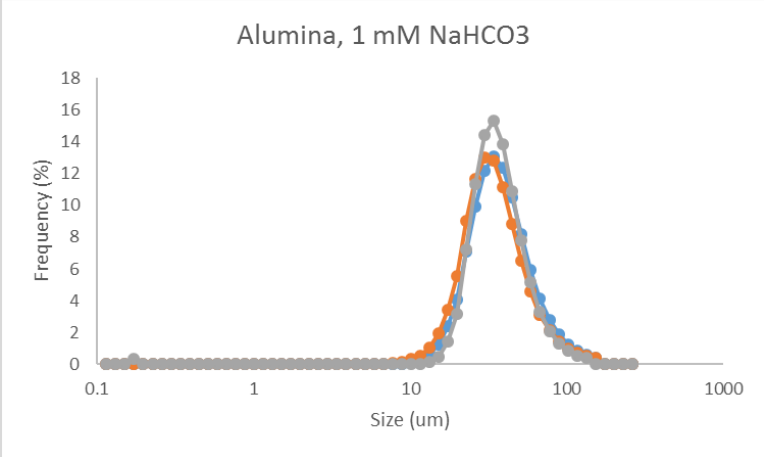

Figure A-32: Alumina particle size distribution in 1 mM $NaHCO_3$ solution

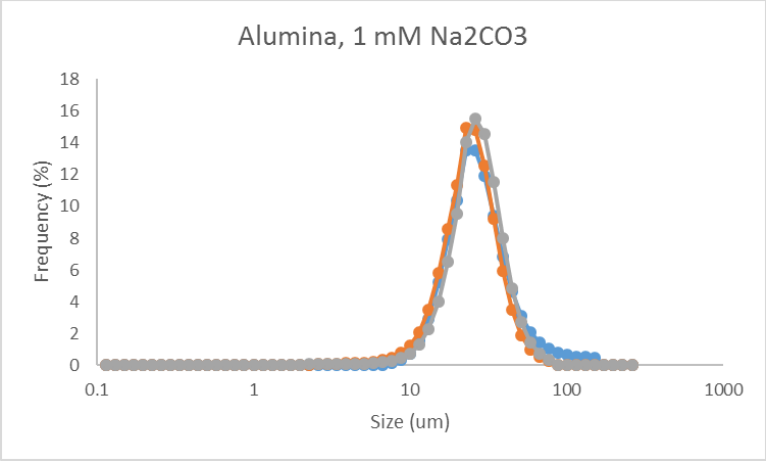

Figure A-33: Alumina particle size distribution in 1 mM Na_2CO_3 solution

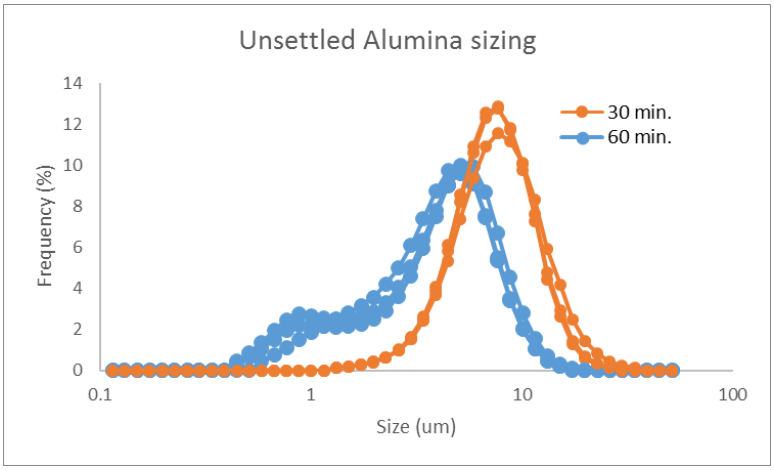

Figure A-34: Particle size distribution on alumina that remained unsettled after 30 and 60 minutes of stagnation in 1 mM Na_2CO_3 solution